Since January 2020 Elsevier has created a COVID-19 resource centre with free information in English and Mandarin on the novel coronavirus COVID-19. The COVID-19 resource centre is hosted on Elsevier Connect, the company's public news and information website.

Journal Pre-proofs

Original article

A new study on two different vaccinated fractional-order COVID-19 models via numerical algorithms

Anwar Zeb, Pushpendra Kumar, Vedat Suat Erturk, Thanin Sitthiwirattham

PII: S1018-3647(22)00095-7
DOI: https://doi.org/10.1016/j.jksus.2022.101914
Reference: JKSUS 101914

To appear in: *Journal of King Saud University - Science*

Received Date: 5 May 2021
Revised Date: 27 September 2021
Accepted Date: 14 February 2022

Please cite this article as: A. Zeb, P. Kumar, V.S. Erturk, T. Sitthiwirattham, A new study on two different vaccinated fractional-order COVID-19 models via numerical algorithms, *Journal of King Saud University - Science* (2022), doi: https://doi.org/10.1016/j.jksus.2022.101914

A new study on two different vaccinated fractional-order COVID-19 models via numerical algorithms

Abstract

The main purpose of this paper is to provide new vaccinated models of COVID-19 in the sense of Caputo-Fabrizio and new generalized Caputo-type fractional derivatives. The formulation of the given models is presented including an exhaustive study of the model dynamics such as positivity, boundedness of the solutions and local stability analysis. Furthermore, the unique solution existence for the proposed fractional order models is discussed via fixed point theory. Numerical solutions are also derived by using two-steps Adams-Bashforth algorithm for Caputo-Fabrizio operator, and modified Predictor-Corrector method for generalised Caputo fractional derivative. Our analysis allow to show that the given fractional-order models exemplify the dynamics of COVID-19 much better than the classical ones. Also, the analysis on the convergence and stability for the proposed methods are performed. By this study, we see that how the vaccine availability plays an important role in the control of COVID-19 infection.

Keywords: Fractional mathematical model, Numerical methods, Caputo-Fabrizio and new generalized Caputo fractional-derivatives
2010 MSC: 26A33, 37N25, 92C60, 92D30

(Version of September 27, 2021)

1. Introduction

Throughout this pandemic known as COVID-19, we have experimented a great expansion of cases throughout the world. This situation converts into solid actions that affect the population: social isolation, use of masks, etc. Mathematical models play a key role for describing infectious diseases such as COVID-19 expansion. The development and investigation of this type of models provide us tools for describing and characterizing its transmission, and thus, we are able to propose successful techniques to foresee, prevent, and control infections, also to ensure that population is well-being. Till present time, numerous mathematical models see [1, 2, 3, 4, 5] have been considered and analyzed to ponder the spreading of infections. COVID-19, has affected nearly 90% countries across the globe with the infection rate rising rapidly at almost 5% per day. However, the COVID-19 infection behavior is different from nation-to-nation, and is depended on numerous factors. In South Africa, with no exception, almost half a million positive cases have been reported already and is currently one of the five most affected countries globally. To date, various mathematical models have been applied to predict infection rates based on only time-series modes [6, 7]. Very few studies attempted to include other related factors to enhancing the modeling process such as the influence of climatic factors for the disease rapid spread. In the last year, numerical models for COVID-19 plague have been taken into consideration by many scientists with respect to

the different nature and its behavior by applying different controls to avoid the spread of this pandemic see [8, 9, 10, 11] and references therein.

Nowadays, number of mathematicians are giving priority to the fractional derivatives [25, 26, 27, 28] in the study of mathematical models. Recently, thousands of epidemic models like tuberculosis [12], malaria [13], COVID-19 [14, 15, 16] have been analyzed by applying non-classical derivative operators. Authors in [17] solved a nonlinear system of COVID-19 by using a recent modification in Caputo derivative. They used fixed point theory techniques to demonstrate solution existence and they also analyzed the stability of the aforementioned model. Dynamics of COVID-19 in Brazil were studied in [18], and in Cameron in [19]. A new model of COVID-19 disease in integer and non-integer sense was provided in ref. [20]. Analysis on the fractional-order mathematical model to simulate the COVID-19 disease outbreaks in Pakistan are proposed in [30]. Authors in [31] have proposed a new non-linear model for deriving the nature of 2019-nCoV. In [32], chaotic dynamics of a mathematical model of HIV-1 in the sense of fractional-order operators is given. In ref. [33], authors have simulated a fractional-order chaotic system. Study proposed in [34] is dedicated to the solution of a fractional-order predator-prey model. In [35], researchers have justified the clear role of prostitutes in the HIV disease. Authors in [36] have analyzed an epidemic model with exponential decay law. In [37], some novel analysis on the listeriosis epidemic are performed. In [38], a modified version of Predictor-Corrector technique for the delay-type fractional differential equations has been proposed. Authors in [39] have analyzed the predictions of COVID-19 cases in Argentina by using a real-data. In [40], researchers have introduced a mathematical model to simulate a biological phenomena. Recently, some authors have also tried fractional derivatives in ecological problems. One of the most recent application is given in [21].

Our objective in this paper is to continue this research line by introducing a new fractional COVID-19 model that takes into account the existence of vaccines. Our paper is organized as follows: Section 2, is related to provide some well-known results that will be later needed. Section 3 is devoted to the description of fractional order models using Caputo-Fabrizio and generalized Caputo non-classical derivatives. Section 4 contains the basic analysis of the model, involving the positivity, boundness, and reproductive number with stability along disease free-equilibrium points. Next, in section 5 and section 6 the existence of solutions for the models via Adams-Bashforth in CF sense and modified Predictor-Corrector in generalized Caputo derivative sense are provided, respectively. These sections also contain the numerical simulations and graphical results for both models. Finally, in section 7, we present the concluding remarks.

2. Preliminaries

Here we mention some definitions and results for further uses.

Definition 1. *[22] The CF (Caputo-Fabrizio) fractional-derivative of $\varkappa$ order for a function $\mathcal{G} \in H^1(c,d)$ and $0 < \varkappa < 1$, is given by:*

$$ {}_c^{CF}D_t^{\varkappa}\mathcal{G}(t) = \frac{1}{1-\kappa}\int_c^t \frac{d\mathcal{G}(\lambda)}{d\lambda} exp[-\varpi(t-\lambda)]d\lambda $$

where $\varpi = \frac{\varkappa}{1-\kappa}$.
The respective CF fractional integral is defined by

$$ {}_c^{CF}I_t^{\varkappa}\mathcal{G}(t) = (1-\varkappa)\mathcal{G}(t) + \varkappa\int_c^t \mathcal{G}(\lambda)d\lambda. $$

Theorem 1. *[23] Let $\mathcal{M}$ be a compact metric space and $C(\mathcal{M},\mathbb{R})$ denotes the space of continuous functions when endowed with the supremum norm metric. A set $\mathcal{E}\subset C(\mathcal{M})$ is compact if and only if $\mathcal{E}$ is bounded, closed and equicontinous.*

Definition 2. *[29] The modified Caputo fractional derivative operator, $D_{d_+}^{\varkappa,\sigma}$, of order $\varkappa>0$ is given by:*

$$(D_{d_+}^{\varkappa,\sigma}\Psi)(\xi)=\frac{\sigma^{\varkappa-n+1}}{\Gamma(n-\varkappa)}\int_d^{\xi}s^{\sigma-1}(\xi^{\sigma}-s^{\sigma})^{n-\varkappa-1}\left(s^{1-\sigma}\frac{d}{ds}\right)^n\Psi(s)ds,\quad \xi>d, \tag{1}$$

where $\sigma>0, d\geq 0,$ and $n-1<\varkappa\leq n$.

Theorem 2. *[29] Let $n-1<\varkappa\leq n,\ \sigma>0,\ a\geq 0$ and $g\in C^n[a,b]$. Then, for $a<t\leq b$,*

$$I_{a+}^{\varkappa,\sigma}D_{a+}^{\varkappa,\sigma}g(t)=g(t)-\sum_{m=0}^{n-1}\frac{1}{\sigma^m m!}(t^{\sigma}-a^{\sigma})^m\left[\left(x^{1-\sigma}\frac{d}{dx}\right)^m g(x)\right]_{x=a}. \tag{2}$$

3. Formulation of fractional-order Covid-19 models

In order to formulate our COVID-19 model with influence of quarantine class and vaccination, we split the whole population into four different compartments. The first of them is the class of susceptible to disease which is represented as $\mathcal{S}_t$, second one is infective or infectious $\mathcal{I}_t$, third one is quarantined $\mathcal{Q}_t$ (in which the infectious peoples are putting for isolation), and last one is the recovered class $\mathcal{R}_t$ with temporary immunity. The flow of the population is described in the following system of differential equations:

$$\begin{aligned}
\frac{d\mathcal{S}_t}{dt}&=(1-q)b-\beta\,\mathcal{S}_t\,\mathcal{I}_t-d\,\mathcal{S}_t+\delta\,\mathcal{R}_t,\\
\frac{d\mathcal{I}_t}{dt}&=\beta\,\mathcal{S}_t\,\mathcal{I}_t-(\eta+\gamma+d+\sigma_1)\,\mathcal{I}_t,\\
\frac{d\mathcal{Q}_t}{dt}&=\eta\,\mathcal{I}_t-(\rho+d+\sigma_2)\,\mathcal{Q}_t,\\
\frac{d\mathcal{R}_t}{dt}&=\gamma\,\mathcal{I}_t+\rho\,\mathcal{Q}_t-(d+\delta)\,\mathcal{R}_t+qb,
\end{aligned} \tag{3}$$

where b describes the enroll rate of the population that directly joins the susceptible class $\mathcal{S}_t$, β stands for the contact rate mainly incidence rate at which susceptible class joins infectious class $\mathcal{I}_t$, d denotes the out going rate of each class in the form of natural death or migration rate from each class, γ is the recovered rate of infected class to join recovered class $\mathcal{R}_t$ and ρ is the recovered rate of quarantine class people. Moreover, σ_1 and σ_2 are the disease related deaths rates for infected class and quarantined class, δ shows the relapse rate at which the recovered class $\mathcal{R}_t$ moves to susceptible class and q represents the vaccine rate, that is, the proportion of the susceptible class that becomes vaccinated with $0\leq q\leq 1$. To simulate the past history or hereditary characteristics in the given model (3), we utilized the Caputo-Fabrizio (CF) fractional derivatives instead of classical derivatives. In this matter, we propose the following model of fractional order type

$$\begin{aligned}
{}_c^{CF}D_t^{\varkappa}\mathcal{S}_t&=(1-q)b-\beta\,\mathcal{S}_t\,\mathcal{I}_t-d\,\mathcal{S}_t+\delta\,\mathcal{R}_t,\\
{}_c^{CF}D_t^{\varkappa}\mathcal{I}_t&=\beta\,\mathcal{S}_t\,\mathcal{I}_t-(\eta+\gamma+d+\sigma_1)\,\mathcal{I}_t,\\
{}_c^{CF}D_t^{\varkappa}\mathcal{Q}_t&=\eta\,\mathcal{I}_t-(\rho+d+\sigma_2)\,\mathcal{Q}_t,\\
{}_c^{CF}D_t^{\varkappa}\mathcal{R}_t&=\gamma\,\mathcal{I}_t+\rho\,\mathcal{Q}_t-(d+\delta)\,\mathcal{R}_t+qb,
\end{aligned} \tag{4}$$

where $0 < \varkappa < 1$ and ${}_c^{CF}D_t^{\varkappa}$ presents the fractional derivative in the Caputo-Fabrizio sense. For generating more diversity in the fractional-order simulations, we propose another fractional order model in the sense of generalized version of Caputo-type fractional derivative as follows:

$$\begin{aligned}
{}^{C}D_t^{\varkappa,\sigma}\mathcal{S}_t &= (1-q)b - \beta\,\mathcal{S}_t\,\mathcal{I}_t - d\,\mathcal{S}_t + \delta\,\mathcal{R}_t,\\
{}^{C}D_t^{\varkappa,\sigma}\mathcal{I}_t &= \beta\,\mathcal{S}_t\,\mathcal{I}_t - (\eta+\gamma+d+\sigma_1)\,\mathcal{I}_t,\\
{}^{C}D_t^{\varkappa,\sigma}\mathcal{Q}_t &= \eta\,\mathcal{I}_t - (\rho+d+\sigma_2)\,\mathcal{Q}_t,\\
{}^{C}D_t^{\varkappa,\sigma}\mathcal{R}_t &= \gamma\,\mathcal{I}_t + \rho\,\mathcal{Q}_t - (d+\delta)\,\mathcal{R}_t + qb,
\end{aligned} \tag{5}$$

where $0 < \varkappa < 1,\ \sigma > 0$, and ${}^{C}D_t^{\varkappa,\sigma}$ prsents the fractional derivative in the generalized (or modified) Caputo sense.

4. Basic analysis of the model

4.1. Positivity and boundedness

Suppose that

$$\mathbb{R}^4_+ = \big\{(\mathcal{S},\mathcal{I},\mathcal{Q},\mathcal{R})|\mathcal{S},\mathcal{I},\mathcal{Q},\mathcal{R} \geq 0\big\}.$$

From [24] and utilizing a generalized mean value theorem and a fractional comparison principle, the proof of the following theorem is achieved. We state the analysis for the Caputo-Fabrizio fractional model (4) and it is straightforward to obtain the corresponding analysis for the generalised Caputo one(5).

Theorem 3 (Positivity and boundedness)**.** *Let $(\mathcal{S}_0,\mathcal{I}_0,\mathcal{Q}_0,\mathcal{R}_0)$ be any initial data belonging to $\mathbb{R}^4_+$ and $\big(\mathcal{S}_t,\mathcal{I}_t,\mathcal{Q}_t,\mathcal{R}_t,\big)$ the corresponding solution of model (4) to the given initial data. The set $\mathbb{R}^4_+$ is positively invariant. Furthermore, we have*

$$\begin{aligned}
\limsup_{t\to\infty}\mathcal{S}_t &\leq \mathcal{S}_\infty := \frac{(1-q)b+\delta\,\mathcal{R}_\infty}{d},\\
\limsup_{t\to\infty}\mathcal{I}_t &\leq \mathcal{I}_\infty := \frac{(1-q)b+\delta\,\mathcal{R}_\infty}{\eta+\gamma+d+\sigma_1},\\
\limsup_{t\to\infty}\mathcal{Q}_t &\leq \mathcal{Q}_\infty := \frac{\eta\,\mathcal{I}_\infty}{\rho+d+\sigma_2},\\
\limsup_{t\to\infty}\mathcal{R}_t &\leq \mathcal{R}_\infty := \frac{\gamma\,\mathcal{I}_\infty+\rho\,\mathcal{Q}_\infty+qb}{d+\delta}.
\end{aligned} \tag{6}$$

Proof. From model (4), we have

$$\begin{aligned}
{}_c^{CF}D_t^{\varkappa}\mathcal{S}\Big|_{\mathcal{S}=0} &= (1-q)b+\delta\,\mathcal{R}_t > 0,\\
{}_c^{CF}D_t^{\varkappa}\mathcal{I}\Big|_{\mathcal{I}=0} &= 0,\\
{}_c^{CF}D_t^{\varkappa}\mathcal{Q}\Big|_{\mathcal{Q}=0} &= \eta\,\mathcal{I}_t \geq 0,\\
{}_c^{CF}D_t^{\varkappa}\mathcal{R}\Big|_{\mathcal{R}=0} &= \gamma\,\mathcal{I}_t+\rho\,\mathcal{Q}_t+qb \geq 0.
\end{aligned} \tag{7}$$

For all $t \geq 0$, with the help of generalized mean value theorem [24] and system (7), we can conclude that $\mathcal{S}_t, \mathcal{I}_t, \mathcal{Q}_t, \mathcal{R}_t \geq 0$. First equation of system (4) implies that

$$ {}_{c}^{CF}D_{t}^{\varkappa}\mathcal{S} \leq (1-q)b - d\,\mathcal{S}_t + \delta\,\mathcal{R}_t. $$

By utilizing the fractional comparison principle, it follows that

$$ \limsup_{t\to\infty} \mathcal{S}_t \leq \mathcal{S}_\infty := \frac{(1-q)b + \delta\,\mathcal{R}_\infty}{d}. $$

Second equation of the system (4) implies that

$$ {}_{c}^{CF}D_{t}^{\varkappa}(\mathcal{S}+\mathcal{I}) \leq (1-q)b - d\,\mathcal{S}_t + \delta\,\mathcal{R}_t - (\eta+\gamma+d+\sigma_1)\,\mathcal{I}_t, $$

which implies that

$$ \limsup_{t\to\infty} \mathcal{I}_t \leq \mathcal{I}_\infty. $$

In a result, the second estimate of (6) is obtained. While third equation of the system (4) gives us

$$ {}_{c}^{CF}D_{t}^{\varkappa}\mathcal{Q} \leq \eta\,\mathcal{I}_\infty - (\rho+d+\sigma_2)\,\mathcal{Q}_t, $$

for enough large value of t. This follows the third estimate of (6).
Finally, the fourth equation of system (4), implies that

$$ {}_{c}^{CF}D_{t}^{\varkappa}\mathcal{R} \leq \gamma\,\mathcal{I}_\infty + \rho\,\mathcal{Q}_\infty - (d+\delta)\,\mathcal{R}_t + qb, $$

for enough large value of t and the fourth estimate of (6) holds. □

4.2. Free virus equilibrium point and reproduction number

Diseases Free Equilibrium (DFE) point of system (3) is given by

$$ \mathcal{E}_0 = \Big(\mathcal{S}_0, \mathcal{I}_0, \mathcal{Q}_0, \mathcal{R}_0\Big) = \left(\frac{b((1-q)d+\delta)}{d(\delta+d)}, 0, 0, \frac{qb}{\delta+d}\right). \tag{8} $$

For the reproductive number of model (3), suppose that $y = (\mathcal{I}_t, \mathcal{S}_t)$ and using next generation matrix approach [3], we have

$$ \frac{dy}{dt} = \mathcal{F}(y) - \mathcal{V}(y), \tag{9} $$

where Jacobian of $\mathcal{F}$ and $\mathcal{V}$ are

$$ \mathcal{F}(y) = \begin{pmatrix} \beta\,\mathcal{S}_t\,\mathcal{I}_t \\ 0 \end{pmatrix} \quad \mathcal{V}(y) = \begin{pmatrix} (\eta+\gamma+d+\sigma_1)\,\mathcal{I}_t \\ -(1-q)b + \beta\,\mathcal{S}_t\,\mathcal{I}_t + d\,\mathcal{S}_t - \delta\,\mathcal{R}_t \end{pmatrix}. \tag{10} $$

At $\mathcal{E}_0$, we have

$$ \mathtt{F}(\mathcal{E}_0) = \begin{pmatrix} \frac{\beta b((1-q)d+\delta)}{d(\delta+d)} & 0 \\ 0 & 0 \end{pmatrix}, \quad \mathtt{V}(\mathcal{E}_0) = \begin{pmatrix} \eta+\gamma+d+\sigma_1 & o \\ \frac{\beta b((1-q)d+\delta)}{d(\delta+d)} & d \end{pmatrix}. $$

Hence, reproductive number for model (3) is

$$ \psi_0 = \rho(\mathtt{F}\mathtt{V}^{-1}) = \frac{\beta b((1-q)d+\delta)}{d(\delta+d)(\eta+\gamma+d+\sigma_1)}. \tag{11} $$

$$\psi_0 = \rho(\mathtt{F}\mathtt{V}^{-1}) = \frac{\beta b((1-q)d+\delta)}{d(\delta+d)(\eta+\gamma+d+\sigma_1)}. \tag{12}$$

The results about the positive endemic equilibrium point are contained in the next theorem.

Theorem 4. *There exists a unique positive endemic equilibrium point $\mathcal{E}^*$ for system (3) if $\psi_0 > 1$.*

Proof. Endemic equilibrium point (EEP) is obtained from system (3), by putting right hand side of each equation equal to zero, we have

$$\begin{aligned}
\mathcal{S}^*{}_t &= \frac{\eta+\gamma+d+\sigma_1}{\beta},\\
\mathcal{Q}^*{}_t &= \frac{\eta}{\rho+d+\sigma_2}\mathcal{I}_t,\\
\mathcal{R}^*{}_t &= \frac{qb}{d+\delta} + \frac{\gamma(\rho+d+\sigma_2)+\rho\eta}{(d+\delta)(\rho+d+\sigma_2)}\mathcal{I}_t,\\
(1-q)b &- (\eta+\gamma+d+\sigma_1)\mathcal{I}^*{}_t - d\,\mathcal{S}^*{}_t + \delta\,\mathcal{R}^*{}_t = 0,
\end{aligned} \tag{13}$$

Now, from last equation of system (13), we have

$$\Phi(\mathcal{I}^*{}_t) = \frac{b((1-q)d+\rho)}{d+\delta} + \left(\frac{\gamma(\rho+d+\sigma_2)+\rho\eta}{(d+\delta)(\rho+d+\sigma_2)} - (\eta+\gamma+d+\sigma_1)\right)\mathcal{I}^*{}_t - \frac{d(\eta+\gamma+d+\sigma_1)}{\beta}. \tag{14}$$

By the values of $\mathcal{S}^*$, $\mathcal{I}^*$, $\mathcal{Q}^*$ and $\mathcal{R}^*$, it is clear that a unique EEP $\mathcal{E}^*$ exists, if $\psi_0 > 1$. □

Theorem 5. *The model (3) is locally stable at $\mathcal{E}_0$ for $\psi_0 < 1$ and unstable for $\psi_0 > 1$.*

Proof. The Jacobian of model (3) is

$$J = \begin{pmatrix} -\beta\mathcal{I}_t - d & -\beta\mathcal{S}_t & 0 & \delta\\ \beta\mathcal{I}_t & \beta\mathcal{S}_t - (\eta+\gamma+d+\sigma_1) & 0 & 0\\ 0 & \eta & -(\rho+d+\sigma_2) & 0\\ 0 & \gamma & \rho & -(d+\delta) \end{pmatrix}. \tag{15}$$

Along $\mathcal{E}_0$, it implies that

$$J(\mathcal{E}_0) = \begin{pmatrix} -d & -\frac{\beta b((1-q)d+\delta)}{d(\delta+d)} & 0 & \delta\\ 0 & \frac{\beta b((1-q)d+\delta)}{d(\delta+d)} - (\eta+\gamma+d+\sigma_1) & 0 & 0\\ 0 & \eta & -(\rho+d+\sigma_2) & 0\\ 0 & \gamma & \rho & -(d+\delta) \end{pmatrix}, \tag{16}$$

which follows that all the eignvalues are negative if $\psi_0 < 1$ and eigenvalue λ_2 is positive for $\psi_0 > 1$. Hence, we conclude that the system (3) is locally stable under the condition $\psi_0 < 1$ and unstable for $\psi_0 > 1$. □

Theorem 6. *The model (3) is globally stable, if $\psi_0 > 1$ at $\mathcal{E}_0$.*

Proof. First, we define the Lyapunov function $\mathcal{V}(t)$, for the system as:

$$\mathcal{V}(t) = 1 + \mathcal{I}_t - \ln \frac{\mathcal{I}_t}{\mathcal{I}_0}. \tag{17}$$

Then differentiating the equation (17) with respect to time, we have

$$\begin{aligned} \frac{d}{dt}(\mathcal{V}(t)) &= \left(1 - \frac{1}{\mathcal{I}_t}\right)\frac{d\mathcal{I}_t}{d(t)} \\ &= \frac{d\mathcal{I}_t}{dt} - \beta\, S_t + (\eta + \gamma + d + \sigma_1). \end{aligned}$$

By manipulating along the point $\mathcal{E}_0$, we get

$$\begin{aligned} \frac{d}{dt}(\mathcal{V}(t)) &= -\left(\beta\, \mathcal{S}_t - (\eta + \gamma + d + \sigma_1)\right) \\ &= -\left(\beta \frac{b((1-q)d + \delta)}{d(\delta + d)} - (\eta + \gamma + d + \sigma_1)\right) \\ &= -(\eta + \gamma + d + \sigma_1)\left(\frac{\beta b((1-q)d + \delta)}{d(\delta + d)(\eta + \gamma + d + \sigma_1)} - 1\right) \\ &\leq 0 \qquad for \quad \psi_0 > 1. \end{aligned}$$

Therefore, if $\psi_0 > 1$, then $\frac{d}{dt}(\mathcal{V}(t) < 0$, which implies that the system (3) is globally stable for $\psi_0 > 1$ at $\mathcal{E}_0$. □

Remark 1. *The simulations of stability of $\mathcal{E}^*$ is an important mathematical term, but in this paper, we particularly focus on the case $\psi_0 < 1$ to find effective manners to prevent the epidemic.*

5. Solution of the variable Caputo-Fabrizio fractional order model (4)

5.1. Existence and uniqueness analysis

Since last few years, a lot of work has been done in the field of existence of solution for different types of fractional differential equations by using techniques from fixed point theory. In order to fulfill this requirement for the proposed model, we use the procedure which has been recently proposed by *Verma et al.* in [23]. For this purpose, we rewrite our model in a compact form given by:

$$\begin{cases} {}^{CF}D_t^{\varkappa}\mathcal{S}_t = \mathcal{G}_1(t, \mathcal{S}_t), \\ {}^{CF}D_t^{\varkappa}\mathcal{I}_t = \mathcal{G}_2(t, \mathcal{I}_t), \\ {}^{CF}D_t^{\varkappa}\mathcal{Q}_t = \mathcal{G}_3(t, \mathcal{Q}_t) \\ {}^{CF}D_t^{\varkappa}\mathcal{R}_t = \mathcal{G}_4(t, \mathcal{R}_t). \end{cases} \tag{18}$$

Now the above system (18) converts to the following fractional Volterra integral form when we apply CF integral operator on it of order $0 < \varkappa < 1$,

$$\begin{aligned}
\mathcal{S}_t(t) - \mathcal{S}_t(0) &= (1-\varkappa)\mathcal{G}_1(t,\mathcal{S}_t) + \varkappa \int_0^t \mathcal{G}_1(\chi,\mathcal{S}_t)d\chi,\\
\mathcal{I}_t(t) - \mathcal{I}_t(0) &= (1-\varkappa)\mathcal{G}_2(t,\mathcal{I}_t) + \varkappa \int_0^t \mathcal{G}_2(\chi,\mathcal{I}_t)d\chi,\\
\mathcal{Q}_t(t) - \mathcal{Q}_t(0) &= (1-\varkappa)\mathcal{G}_3(t,\mathcal{Q}_t) + \varkappa \int_0^t \mathcal{G}_3(\chi,\mathcal{Q}_t)d\chi,\\
\mathcal{R}_t(t) - \mathcal{R}_t(0) &= (1-\varkappa)\mathcal{G}_4(t,\mathcal{R}_t) + \varkappa \int_0^t \mathcal{G}_4(\chi,\mathcal{R}_t)d\chi.
\end{aligned} \tag{19}$$

Now we derive the analysis for $\mathcal{S}_t(t)$ and it is straightforward to mention that the given analysis will exist in a similar way for the other model equations of (18).
Consider the Banach space $\mathcal{B} = C([0,T])$ with the associated norm $\| \mathcal{S}_t \| = \max_{t\in[0,T]}\{|\mathcal{S}_t|, \forall \mathcal{S}_t \in \mathcal{B}\}$ and $\varkappa^* = \min_{t\in[0,T]}\{\varkappa\}$ and $\varkappa^{**} = \max_{t\in[0,T]}\{\varkappa\}$ be the minimum and maximum weight of the variable non-integer order $\varkappa$ on $[0,T]$. Now, we recall the following hypothesis to explore our main observations:
$[\mathcal{X}_1]$: There exist constants $\mathcal{G}_c, H_c > 0$, and $k \in [0,1)$ such that $|\mathcal{G}_1(t,\mathcal{S}_t)| \leq \mathcal{G}_c|\mathcal{S}_t|^k + H_c$.
$[\mathcal{X}_2]$: There exists a constant $N_c > 0$, such that $|\mathcal{G}_1(t,\mathcal{S}_{t_1}) - \mathcal{G}_1(t,\mathcal{S}_{t_2})| \leq N_c|\mathcal{S}_{t_1}(t) - \mathcal{S}_{t_2}(t)|$.
Now, we define the operator $\mathcal{O} : \mathcal{B} \to \mathcal{B}$ as

$$\mathcal{O}(\mathcal{S}_t(t)) = \mathcal{S}_t(0) + (1-\varkappa)\mathcal{G}_1(t,\mathcal{S}_t) + \varkappa \int_0^t \mathcal{G}_1(\chi,\mathcal{S}_t)d\chi. \tag{20}$$

It is clear that operator $\mathcal{O}(\mathcal{S}_t(t)) = \mathcal{O}_1(\mathcal{S}_t(t)) + \mathcal{O}_2(\mathcal{S}_t(t))$, where

$$\mathcal{O}_1(\mathcal{S}_t(t)) = \mathcal{S}_t(0) + (1-\varkappa)G_1(t,\mathcal{S}_t). \tag{21}$$

$$\mathcal{O}_2(\mathcal{S}_t(t)) = \varkappa \int_0^t \mathcal{G}_1(\chi,\mathcal{S}_t)d\chi. \tag{22}$$

Theorem 7. *Assume that hypothesis $[\mathcal{X}_2]$ holds and there exists $\mathcal{C} > 0$ (constant) such that $\mathcal{C} = [(1-\varkappa^*)N_c + \varkappa^* N_c T] < 1$. Then $\mathcal{O}$ has a unique fixed point for the model (18) on $\mathcal{B}$.*

Proof. Let consider $\mathcal{S}_{t_1}, \mathcal{S}_{t_2} \in \mathcal{B}$. Then

$$\begin{aligned}
&\| \mathcal{O}\mathcal{S}_{t_1} - \mathcal{O}\mathcal{S}_{t_2} \| \leq \| \mathcal{O}_1\mathcal{S}_{t_1} - \mathcal{O}_1\mathcal{S}_{t_2} \| + \| \mathcal{O}_2\mathcal{S}_{t_1} - \mathcal{O}_2\mathcal{S}_{t_2} \|\\
&\leq (1-\varkappa) \max_{t\in[0,T]} |\mathcal{G}_1(t,\mathcal{S}_{t_1}) - G_1(t,\mathcal{S}_{t_2})|\\
&+ \varkappa \max_{t\in[0,T]} | \int_0^t \mathcal{G}_1(\xi,\mathcal{S}_{t_1})d\xi - \int_0^t \mathcal{G}_1(\xi,\mathcal{S}_{t_1})d\xi|\\
&\leq [(1-\varkappa)N_c + \varkappa N_c T] \max_{t\in[0,T]} |\mathcal{S}_{t_1} - \mathcal{S}_{t_2}|\\
&\leq [(1-\varkappa^*)N_c + \varkappa^* N_c T] \| \mathcal{S}_{t_1} - \mathcal{S}_{t_2} \|\\
&\leq \mathcal{C} \| \mathcal{S}_{t_1} - \mathcal{S}_{t_2} \| .
\end{aligned} \tag{23}$$

Since $\mathcal{C} = [(1-\varkappa^*)N_c + \varkappa^* N_c T] < 1$, using Banach fixed point theorem, we conclude that the operator $\mathcal{O}$ has a unique fixed point. Then, the model (18) has a unique solution. □

Theorem 8. *Assume that statements* $[\mathcal{X}_1]-[\mathcal{X}_2]$ *hold and* $0<(1-\varkappa^*)N_c<1$. *Then the system* (18) *has at least one solution.*

Proof. First, we show the operator $\mathcal{O}_1$ is a contraction. Indeed, it is given $\mathcal{S}_t \in \mathcal{T}$ where $\mathcal{T}=\{\mathcal{S}_t \in \mathcal{B} :\| \mathcal{S}_t \| \leq w, w>0\}$ is a closed convex set it follows that

$$\| \mathcal{O}_1\mathcal{S}_{t_1}-\mathcal{O}_1\mathcal{S}_{t_2} \| = (1-\varkappa) \max_{t\in[0,T]} |\mathcal{G}_1(t,\mathcal{S}_{t_1})-\mathcal{G}_1(t,\mathcal{S}_{t_2})| \leq [(1-\varkappa^*)N_c \| \mathcal{S}_{t_1}-\mathcal{S}_{t_2} \| . \quad (24)$$

Hence $\mathcal{O}_1$ is a contraction. Now to demonstrate that the second operator O_2 is compact we can see that O_2 is continuous and compact for any $\mathcal{S}_t \in \mathcal{T}$, then $\mathcal{O}_2$ is contraction as $\mathcal{G}_1$ is continuous, then

$$\| \mathcal{O}_2\mathcal{S}_t(t) \| = \max_{t\in[0,T]} |\varkappa \int_0^t \mathcal{G}_1(\xi,\mathcal{S}_t)d\xi| \leq |\varkappa| \int_0^t |\mathcal{G}_1(\xi,\mathcal{S}_t)|d\xi \leq \varkappa^* T[\mathcal{G}_c|\mathcal{S}_t|^k + H_c]. \quad (25)$$

So, $\mathcal{O}_2$ is bounded. Now, assume $t_1>t_2 \in [0.T]$, such that

$$\| \mathcal{O}_2\mathcal{S}_t(t_1)-\mathcal{O}_2\mathcal{S}_t(t_2) \| = \varkappa^* \max_{t\in[0,T]} | \int_0^{t_1} \mathcal{G}_1(\xi,\mathcal{S}_t)d\xi - \int_0^{t_2} \mathcal{G}_1(\xi,\mathcal{S}_t)d\xi| \leq \varkappa^*[\mathcal{G}_c|\mathcal{S}_t|^k + H_c]|t_1-t_2|. \quad (26)$$

This yields $\| \mathcal{O}_2(\mathcal{S}_t(t_1))-\mathcal{O}_2(\mathcal{S}_t(t_2)) \| \to 0$ as $t_1 \to t_2$. Hence, the operator $\mathcal{O}_2$ is equicontinuous. As a consequence of Theorem 1, $\mathcal{O}_2$ is compact. Now by referring to the analysis given in section 5 of *Verma et al.* [23], we concludes that the given system has at least one solution. □

5.2. Numerical solution of CF system

Now we write the solution of the proposed system in CF sense applying two-step Adams-Bashforth algorithm. Our time interval is $[a,T]$ with the step width $h=\frac{T-a}{N}$, where N is the sample size.

Let $\mathcal{S}_{t_j}$ be the numerical approximation of $\mathcal{S}_t(t)$ at $t=t_j$, where $t_j=0+jh$ and $j=0,1,...,N$. Writing the equations of $\mathcal{S}_t(t)$ at the uniform grid points $(t_0,t_1,t_2,...,t_{j-1},t_j,t_{j+1})$, we get the estimations at distinct grid point values. For doing it, first we consider the equivalent Volterra CF integral equation for $\mathcal{S}_t(t)$ which is,

$$\mathcal{S}_t(t)=\mathcal{S}_t(0)+(1-\varkappa)\mathcal{G}_1(t,\mathcal{S}_t(t))+\varkappa\int_0^t \mathcal{G}_1(s,\mathcal{S}_t(s))ds. \quad (27)$$

So the estimations at t_j are

$$\mathcal{S}_t(t_j)=\mathcal{S}_{t_0}+(1-\varkappa)\mathcal{G}_1(t_{j-1},\mathcal{S}_t(t_{j-1}))+\varkappa\int_0^{t_j} \mathcal{G}_1(t,\mathcal{S}_t(t))dt, \quad (28)$$

and at t_{j+1}

$$\mathcal{S}_t(t_{j+1})=\mathcal{S}_{t_0}+(1-\varkappa)\mathcal{G}_1(t_j,\mathcal{S}_t(t_j))+\varkappa\int_0^{t_{j+1}} \mathcal{G}_1(t,\mathcal{S}_t(t))dt. \quad (29)$$

Subtracting equation (29) from (28), we get

$$\mathcal{S}_t(t_{j+1})-\mathcal{S}_t(t_j)=(1-\varkappa)\left(\mathcal{G}_1(t_j,\mathcal{S}_t(t_j))-\mathcal{G}_1(t_{j-1},\mathcal{S}_t(t_{j-1}))\right)+\varkappa\int_{t_j}^{t_{j+1}} \mathcal{G}_1(t,\mathcal{S}_t(t))dt. \quad (30)$$

Now, by applying linear interpolation to $\mathcal{G}_1(t, \mathcal{S}_t(t))$ and employing trapezoid rule on the integral part, we obtain

$$\int_{t_j}^{t_{j+1}} \mathcal{G}_1(t, \mathcal{S}_t(t))dt \approxeq \frac{3\Delta t}{2}\mathcal{G}_1(t_j, \mathcal{S}_t(t_j)) - \frac{\Delta t}{2}\mathcal{G}_1(t_j, \mathcal{S}_t(t_j)), \tag{31}$$

where $\Delta t = t_j - t_{j-1}$. Hence, we have established the numerical approximation for $\mathcal{S}_t(t)$ as

$$\mathcal{S}_t(t_{j+1}) = \mathcal{S}_t(t_j) + \left(1 - \varkappa + \frac{3\varkappa\Delta t}{2}\right)\mathcal{G}_1(t_j, \mathcal{S}_t(t_j)) - \left(1 - \varkappa + \frac{\varkappa\Delta t}{2}\right)\mathcal{G}_1(t_{j-1}, \mathcal{S}_t(t_{j-1})). \tag{32}$$

As a consequence, the solution of the proposed CF model (18) states as follows:

$$\begin{aligned}
\mathcal{S}_t(t_{j+1}) &= \mathcal{S}_t(t_j) + \left(1 - \varkappa + \frac{3\varkappa\Delta t}{2}\right)\mathcal{G}_1(t_j, \mathcal{S}_t(t_j)) - \left(1 - \varkappa + \frac{\varkappa\Delta t}{2}\right)\mathcal{G}_1(t_{j-1}, \mathcal{S}_t(t_{j-1})),\\
\mathcal{I}_t(t_{j+1}) &= \mathcal{I}_t(t_j) + \left(1 - \varkappa + \frac{3\varkappa\Delta t}{2}\right)\mathcal{G}_2(t_j, \mathcal{I}_t(t_j)) - \left(1 - \varkappa + \frac{\varkappa\Delta t}{2}\right)\mathcal{G}_2(t_{j-1}, \mathcal{I}_t(t_{j-1})),\\
\mathcal{Q}_t(t_{j+1}) &= \mathcal{Q}_t(t_j) + \left(1 - \varkappa + \frac{3\varkappa\Delta t}{2}\right)\mathcal{G}_3(t_j, \mathcal{Q}_t(t_j)) - \left(1 - \varkappa + \frac{\varkappa\Delta t}{2}\right)\mathcal{G}_3(t_{j-1}, \mathcal{Q}_t(t_{j-1})),\\
\mathcal{R}_t(t_{j+1}) &= \mathcal{R}_t(t_j) + \left(1 - \varkappa + \frac{3\varkappa\Delta t}{2}\right)\mathcal{G}_4(t_j, \mathcal{R}_t(t_j)) - \left(1 - \varkappa + \frac{\varkappa\Delta t}{2}\right)\mathcal{G}_4(t_{j-1}, \mathcal{R}_t(t_{j-1})).
\end{aligned} \tag{33}$$

Theorem 9. *The proposed numerical scheme* (32) *is unconditionally stable if (particularly for first model equation)*

$$\|\mathcal{G}_1(t_{j+1}, \mathcal{S}_t(t_{j+1})) - \mathcal{G}_1(t_j, \mathcal{S}_t(t_j))\| \to 0.$$

Proof. Given $\mathcal{S}_t(t)$ the solution of (27), we have that:

$$\begin{aligned}
\|\mathcal{S}_t(t_{j+1}) - \mathcal{S}_t(t_j)\| &= \left\|(1-\varkappa)\left(\mathcal{G}_1(t_j, \mathcal{S}_t(t_j)) - \mathcal{G}_1(t_{j-1}, \mathcal{S}_t(t_{j-1}))\right) + \varkappa\int_{t_j}^{t_{j+1}} \mathcal{G}_1(\eta, \mathcal{S}_t(\eta))d\eta\right\|\\
&\leq (1-\varkappa)\left\|\left(\mathcal{G}_1(t_j, \mathcal{S}_t(t_j)) - \mathcal{G}_1(t_{j-1}, \mathcal{S}_t(t_{j-1}))\right)\right\| + \varkappa\left\|\int_{t_j}^{t_{j+1}} \mathcal{G}_1(\eta, \mathcal{S}_t(\eta))d\eta\right\|.
\end{aligned} \tag{34}$$

Making $j \to \infty$, we get

$$\begin{aligned}
\|\mathcal{S}_t(t_{j+1}) - \mathcal{S}_t(t_j)\|_\infty &\leq \lim_{j\to\infty}(1-\varkappa)\left\|\left(\mathcal{G}_1(t_j, \mathcal{S}_t(t_j)) - \mathcal{G}_1(t_{j-1}, \mathcal{S}_t(t_{j-1}))\right)\right\| + \lim_{j\to\infty}\varpi\left\|\int_{t_j}^{t_{j+1}} \mathcal{G}_1(\eta, \mathcal{S}_t(\eta))d\eta\right\|\\
&< \lim_{j\to\infty}(1-\varkappa)\left\|\left(\mathcal{G}_1(t_j, P(t_j)) - \mathcal{G}_1(t_{j-1}, \mathcal{S}_t(t_{j-1}))\right)\right\|\\
&\quad + \lim_{j\to\infty}\varkappa\int_{t_j}^{t_{j+1}}\left|\sum_{j=0}^{j}\prod_{j=0}^{j}\frac{\eta - t_j}{\Delta t}\mathcal{G}_1(t_j, \mathcal{S}_t(t_j))\right|d\eta
\end{aligned}$$

Clearly, the second part of the above inequality goes to zero when $j \to \infty$. Now, if $||\mathcal{G}_1(t_{j+1}, \mathcal{S}_t(t_{j+1})) - \mathcal{G}_1(t_j, \mathcal{S}_t(t_j))|| \to 0$ as $j \to \infty$, we conclude that the given scheme is stable. □

Theorem 10 (Convergence). *Let the solution of ${}^{CF}D_t^{\varkappa} S_t(t)$ be $S_t(t)$. Then there exist Γ, such that $\left\|\mathbb{O}_{\varkappa}^{k}\right\| \leq \Gamma$.*

Proof. Starting from equation (30) and performing linear interpolation, we have

$$\begin{aligned} S_t(t_{j+1}) - S_t(t_j) &= (1-\varkappa)\left(G_1(t_j, S_t(t_j)) - G_1(t_{j-1}, S_t(t_{j-1}))\right) + \varkappa \int_{t_j}^{t_{j+1}} G_1(\eta, S_t(\eta))d\eta \\ &= (1-\varkappa)\left(G_1(t_j, S_t(t_j)) - G_1(t_{j-1}, S_t(t_{j-1}))\right) \\ &\quad + \varkappa \int_{t_j}^{t_{j+1}} \left\{ G_1(t_j, S_t(t_j)) \left(\frac{\eta - t_{j-1}}{\Delta t}\right) - G_1(t_{j-1}, S_t(t_{j-1})) \left(\frac{\eta - t_j}{\Delta t}\right) \right\} d\eta \\ &\quad + \varkappa \int_{t_j}^{t_{j+1}} \left\{ \sum_{a=0}^{j-2} \prod_{a=0}^{j-2} G_1(t_a, S_t(t_a)) \left(\frac{\eta - t_a}{(-1)^a \Delta_a}\right) \right\} d\eta \end{aligned} \tag{35}$$

Simplifying further, we arrive at the numerical solution with the truncation term

$$S_t(t_{j+1}) = S_t(t_j) + \left(1 - \varkappa + \frac{3\varkappa\Delta t}{2}\right) G_1(t_j, S_t(t_j)) + \left(1 - \varkappa + \frac{\varkappa\Delta t}{2}\right) G_1(t_{j-1}, S_t(t_{j-1})) + \mathbb{O}_{\varkappa}^{j} \tag{36}$$

where the truncation term is written as

$$\mathbb{O}_{\varkappa}^{j} = \varkappa \int_{t_j}^{t_{j+1}} \left\{ \sum_{a=0}^{j-2} \prod_{a=0}^{j-2} G_1(t_a, S_t(t_a)) \left(\frac{\eta - t_a}{(-1)^a \Delta t_a}\right) \right\} d\eta \tag{37}$$

Then taking the norm, we have

$$\begin{aligned} \left\|\mathbb{O}_{\varkappa}^{j}\right\| &= \left\| \varkappa \int_{t_j}^{t_{j+1}} \left\{ \sum_{a=0}^{j-2} \prod_{a=0}^{j-2} G_1(t_a, S_t(t_a)) \left(\frac{\eta - t_a}{(-1)^a \Delta t_a}\right) \right\} d\eta \right\| \\ &\leq \varkappa \int_{t_j}^{t_{j+1}} \left\| \left\{ \sum_{a=0}^{j-2} \prod_{a=0}^{j-2} G_1(t_a, S_t(t_a)) \left(\frac{\eta - t_a}{(-1)^a \Delta t_a}\right) \right\} d\eta \right\| \\ &< \varkappa \int_{t_j}^{t_{j+1}} \sum_{a=0}^{j-2} \prod_{a=0}^{j-2} \left| \frac{\eta - t_a}{\Delta t_a} \right| \sup_a \left(\max_a \left| G_1(t_a, S_t(t_a)) \right| \right) d\eta \\ &< \varkappa (j-1)! \Delta t^{j-1} \Gamma \end{aligned} \tag{38}$$

Hence, the solution has a convergence result. □

5.3. Graphical simulations

In this section, we derive the all necessary plots by using the above given scheme. We use the initial populations $\mathcal{S}_t(0) = 100$, $\mathcal{I}_t(0) = 10$, $\mathcal{Q}_t(0) = 5$, $\mathcal{R}_t(0) = 0$, and parameter values $d = 0.001$, $\beta = 0.003$, $\delta = 0.003$, $\gamma = 0.002$, $b = 10$, $\eta = 0.05$, $\rho = 0.003$, $\sigma_1 = 0.003$, $\sigma_2 = 0.002$, $q = 1$(this value is just an assumption) which are taken from the literature of COVID-19 cases in China [14, 17]. In the collection of Figure 1, the subfigures 1a, 1b, 1c, 1d are devoted to show the variations in $\mathcal{S}_t, \mathcal{I}_t, \mathcal{Q}_t$, and $\mathcal{R}_t$ against the time variable t. Here, the variations in the dynamics of the model can be clearly explored at different derivative order values. We can observe that when the fractional order values changes then the differences

between phases of the plot lines increases. Figure 2 reflects the relations between the given classes. Subfigure 2a plots the variations of $\mathcal{S}_t$ versus $\mathcal{I}_t$, subfigure 2b plots the corresponding ones for $\mathcal{S}_t$ versus $\mathcal{Q}_t$ and 2c plots the variations of $\mathcal{S}_t$ versus $\mathcal{R}_t$. Finally, subfigure 2d plots $\mathcal{R}_t$ against $\mathcal{I}_t$. The fractional order values which have been considered are $\varkappa = 0.75, 0.85, 0.95, 1$.

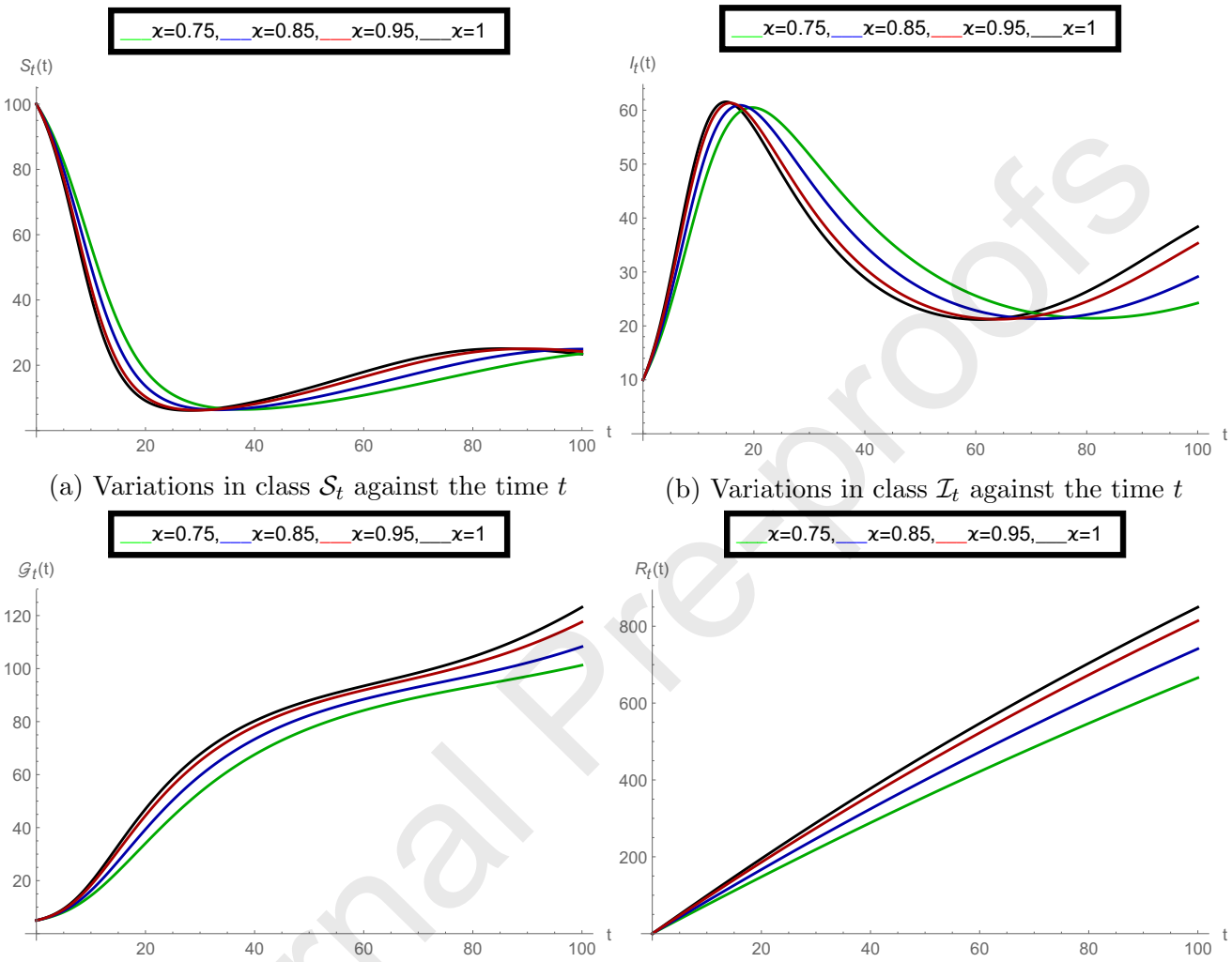

(a) Variations in class $\mathcal{S}_t$ against the time t

(b) Variations in class $\mathcal{I}_t$ against the time t

(c) Variations in class $\mathcal{Q}_t$ against the time t

(d) Variations in class $\mathcal{R}_t$ against the time t

Figure 1: Structure of the model classes in CF sense at various values of order $\varkappa$, when vaccination fraction $q = 1$.

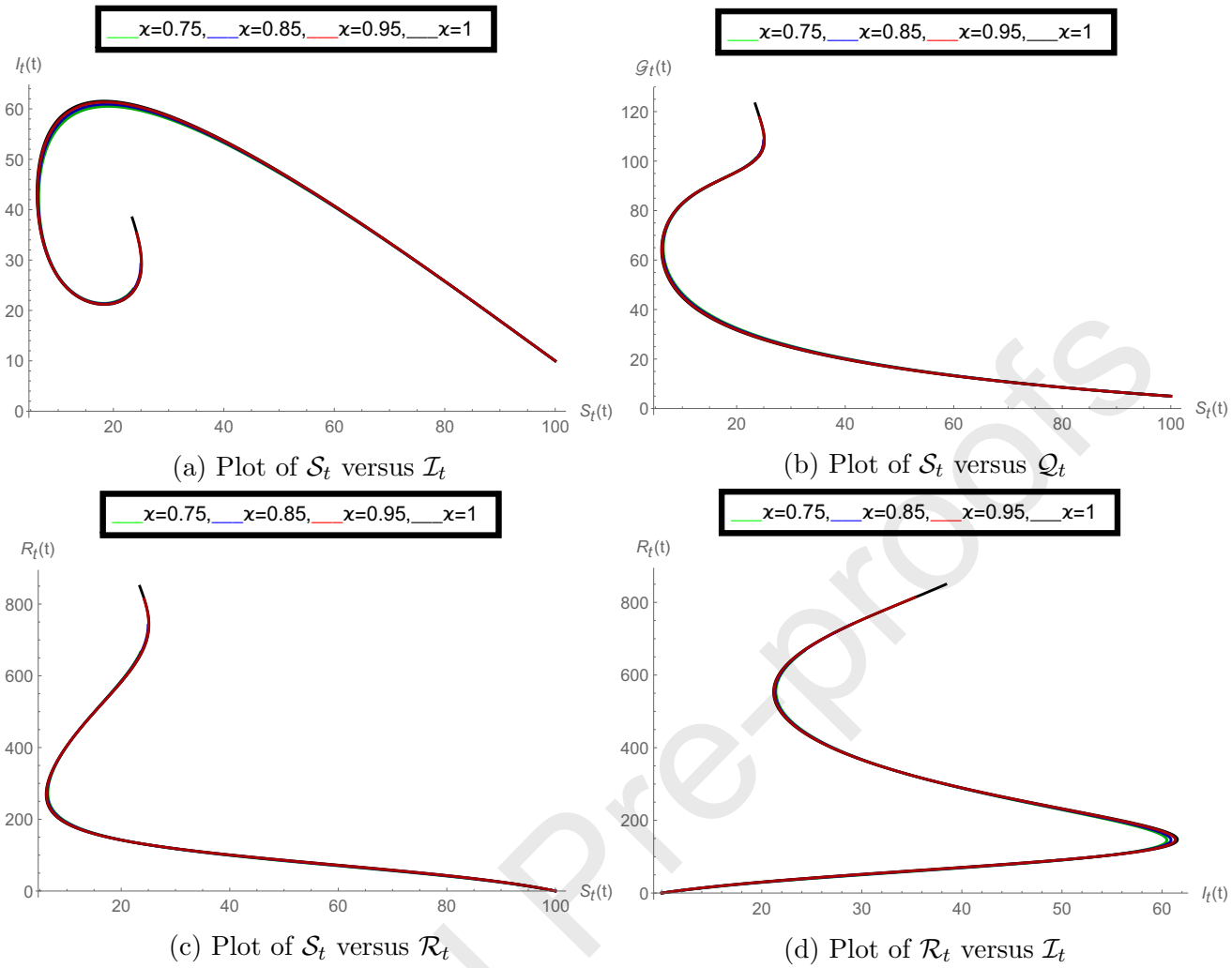

(a) Plot of $\mathcal{S}_t$ versus $\mathcal{I}_t$

(b) Plot of $\mathcal{S}_t$ versus $\mathcal{Q}_t$

(c) Plot of $\mathcal{S}_t$ versus $\mathcal{R}_t$

(d) Plot of $\mathcal{R}_t$ versus $\mathcal{I}_t$

Figure 2: Variations in the model classes compare to each other, when vaccination fraction $q = 1$.

Now we intend to explore the role of vaccine on the given model classes. For this purpose, we change the value of the vaccination fraction q to simulate the model structure. Here, in the family of Figure 3, the subfigures 3a, 3b, 3c, 3d demonstrate the variations in $\mathcal{S}_t, \mathcal{I}_t, \mathcal{Q}_t$, and $\mathcal{R}_t$ against the time variable t at the vaccination fraction $q = 0$, where all other values are same as used above. Similarly, Figure 4 shows the corresponding ones when the vaccination fraction $q = 0.5$. By the comparison of these figures, we can easily observe that when the value of vaccination fraction q increases then the population of infectious humans decreases. So, vaccine availability is one of the most important control measure to reduce the infection of COVID-19.

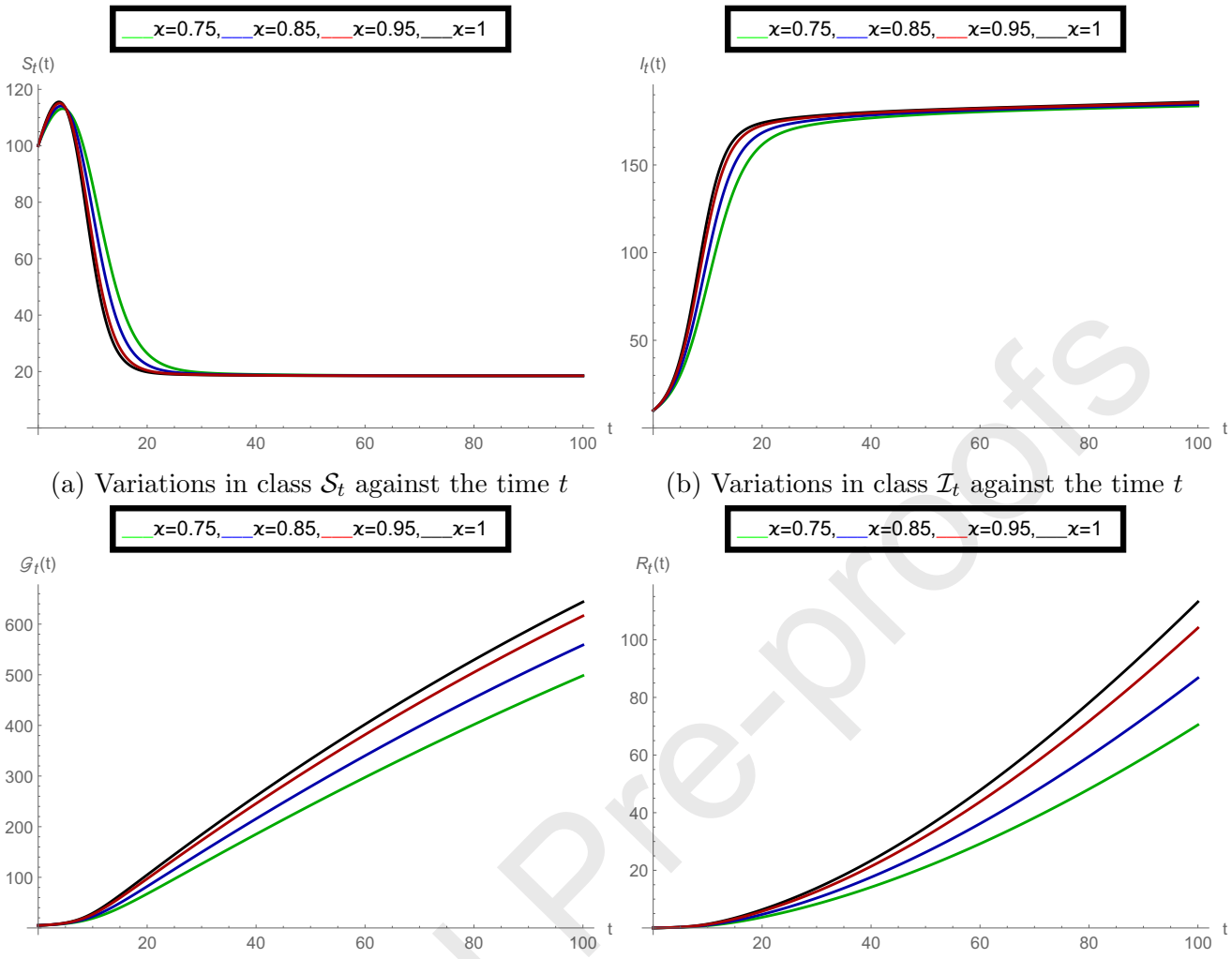

(a) Variations in class $\mathcal{S}_t$ against the time t

(b) Variations in class $\mathcal{I}_t$ against the time t

(c) Variations in class $\mathcal{Q}_t$ against the time t

(d) Variations in class $\mathcal{R}_t$ against the time t

Figure 3: Structure of the model classes in CF sense at various values of order $\varkappa$, when vaccination fraction $q = 0$.

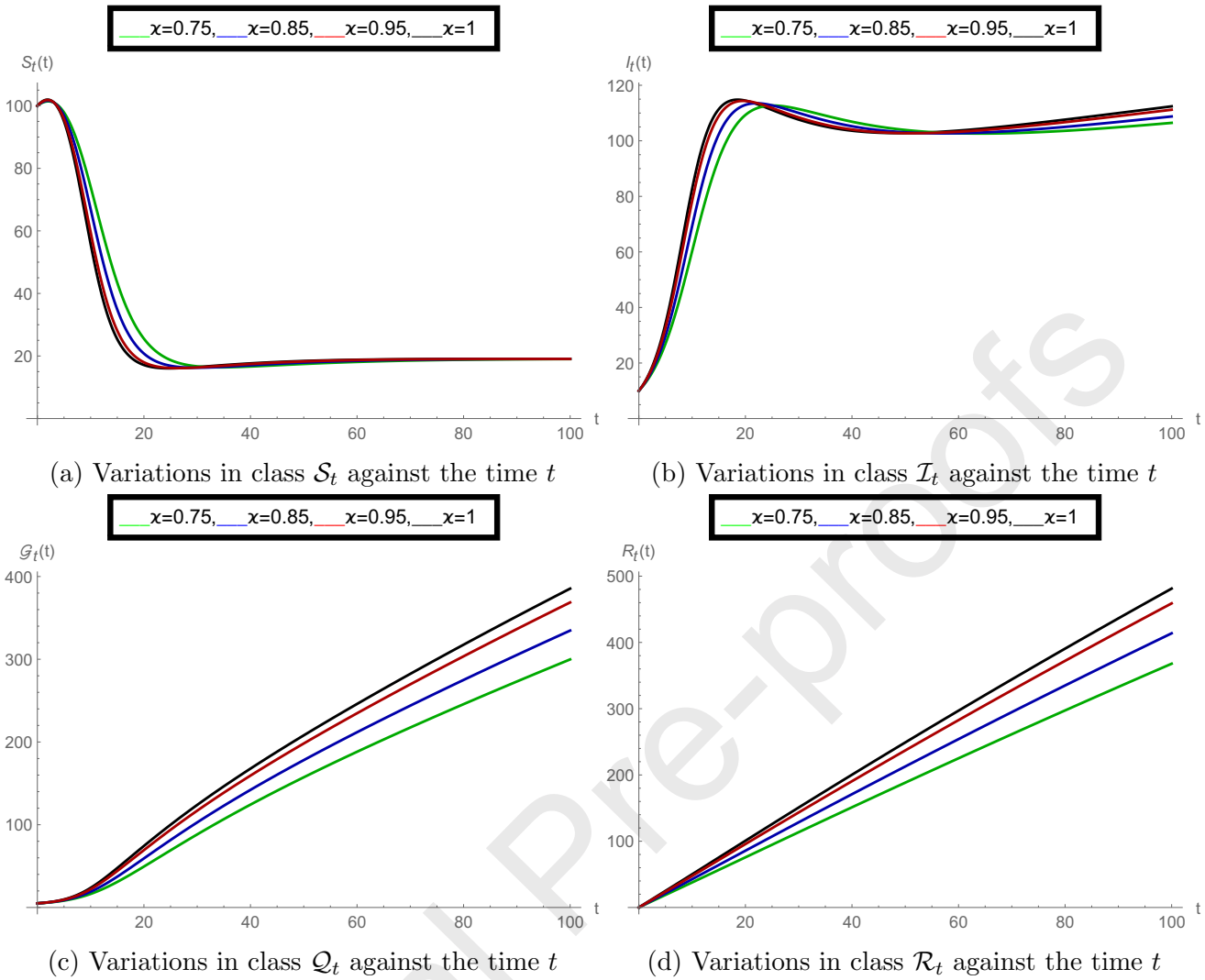

(a) Variations in class $\mathcal{S}_t$ against the time t

(b) Variations in class $\mathcal{I}_t$ against the time t

(c) Variations in class $\mathcal{Q}_t$ against the time t

(d) Variations in class $\mathcal{R}_t$ against the time t

Figure 4: Structure of the model classes in CF sense at various values of order $\varkappa$, when vaccination fraction $q = 0.5$.

6. Solution of the generalised Caputo fractional model (5)

6.1. Existence and uniqueness analysis

In this concern, to prove the existence of unique solution of the proposed modified Caputo type fractional order model, we again write the given model into compact form as

$$\begin{cases} {}^{C}D_t^{\varkappa,\sigma}\mathcal{S}_t = \mathcal{G}_1(t,\mathcal{S}_t), \\ {}^{C}D_t^{\varkappa,\sigma}\mathcal{I}_t = \mathcal{G}_2(t,\mathcal{I}_t), \\ {}^{C}D_t^{\varkappa,\sigma}\mathcal{Q}_t = \mathcal{G}_3(t,\mathcal{Q}_t) \\ {}^{C}D_t^{\varkappa,\sigma}\mathcal{R}_t = \mathcal{G}_4(t,\mathcal{R}_t). \end{cases} \tag{39}$$

Now we just adopt the first equation of the above system to derive the necessary results.

$${}^{C}D_t^{\varkappa,\sigma}\mathcal{S}_t(t) = \mathcal{G}_1(t,\mathcal{S}_t), \tag{40a}$$

$$\mathcal{S}_t(0) = \mathcal{S}_{t_0}. \tag{40b}$$

The equivalent Volterra integral equation of the proposed IVP is

$$\mathcal{S}_t(t) = \mathcal{S}_t(0) + \frac{\sigma^{1-\varkappa}}{\Gamma(\varkappa)} \int_0^t \xi^{\sigma-1}(t^\sigma - \xi^\sigma)^{\varkappa-1} \mathcal{G}_1(\xi, \mathcal{S}_t) d\xi. \tag{41}$$

Theorem 11. *[17] (Existence). Let $0 < \varkappa \leq 1$, $N_0 \in \mathbb{R}$, $K > 0$ and $T^* > 0$. Let $\mathcal{G} := \{(t, \mathcal{S}_t) : \ t \in [0, T^*], \ |\mathcal{S}_t - \mathcal{S}_{t_0}| \leq K\}$ and take the function $\mathcal{G}_1 : \mathcal{G} \to \mathbb{R}$ be continuous. Further, describe $M := \sup_{(t,\mathcal{S}_t)\in\mathcal{G}} |\mathcal{G}_1(t, \mathcal{S}_t)|$ and*

$$T = \begin{cases} T^*, & \text{if } M = 0, \\ min\left\{T^*, \left(\dfrac{K\Gamma(\varkappa+1)\sigma^\varkappa}{M}\right)^{\frac{1}{\varkappa}}\right\} & \text{otherwise.} \end{cases} \tag{42}$$

Then, there exists a function $\mathcal{S}_t \in C[0, T]$ that satisfies the IVP (40a) *and* (40b).

Lemma 1. *[17] If the assumptions of the statement of Theorem 1 hold, the function $\mathcal{S}_t \in C[0, T]$ satisfies the IVP* (40a) *and* (40b) *if and only if it satisfies the non-linear Volterra integral equation* (41).

Theorem 12. *[17] (Uniqueness). Consider $\mathcal{S}_t(0) \in \mathbb{R}$, $K > 0$ and $T^* > 0$. Also, let $0 < \varkappa \leq 1$ and $m = \lceil \varkappa \rceil$. For the set $\mathcal{G}$ as given in Theorem 9 and assume $\mathcal{G}_1 : \mathcal{G} \to \mathbb{R}$ be continuous. Assume that $\mathcal{G}_1$ agrees to the Lipschitz condition with respect to the second variable, i.e.*

$$|\mathcal{G}_1(t, \mathcal{S}_{t_1}) - \mathcal{G}_1(t, \mathcal{S}_{t_2})| \leq V|\mathcal{S}_{t_1} - \mathcal{S}_{t_2}|,$$

for some constant $V > 0$ which does not dependent to $t, \mathcal{S}_{t_1}$, and $\mathcal{S}_{t_2}$. Then, a unique solution $\mathcal{S}_t \in C[0, T]$ exists for the IVP (40a) *and* (40b).

6.2. Derivation of the solution via modified Predictor-Corrector algorithm

Now we construct the numerical solution of the proposed Caputo fractional model using a modified form of the PC algorithm as mentioned in [29] with some appropriate changes. Here we start with Volterra integral equation (41), which provides

$$\mathcal{S}_t(t) = \mathcal{S}_t(0) + \frac{\sigma^{1-\varkappa}}{\Gamma(\varkappa)} \int_0^t \xi^{\sigma-1}(t^\sigma - \xi^\sigma)^{\varkappa-1} \mathcal{G}_1(\xi, \mathcal{S}_t) d\xi, \tag{43}$$

Here, first we recall that a unique solution of the proposed model exists under suitable conditions on the function $\mathcal{G}_1$ on some interval $[0, T]$. We divide the interval $[0, T]$ into N non-uniform subintervals $\{[t_k, t_{k+1}], \ k = 0, 1, ..., N-1\}$ taking the mesh points

$$\begin{cases} t_0 = 0, \\ t_{k+1} = (t_k^\sigma + h)^{1/\sigma}, \quad k = 0, 1, ..., \mathbb{N} - 1, \end{cases} \tag{44}$$

here $h = \dfrac{T^\sigma}{\mathbb{N}}$. We now analyse the approximations $\mathcal{S}_{t_k}$, $k = 0, 1, ..., \mathbb{N}$, to solve numerically the proposed IVP. First of all, assuming the approximation $\mathcal{S}_{t_j} \approx \mathcal{S}_t(t_j)(j = 1, 2, ..., k)$, we estimate $\mathcal{S}_{t_{k+1}} \approx \mathcal{S}_t(t_{k+1})$ by means of the integral equation

$$\mathcal{S}_t(t_{k+1}) = \mathcal{S}_t(0) + \frac{\sigma^{1-\varkappa}}{\Gamma(\varkappa)} \int_0^{t_{k+1}} \xi^{\sigma-1}(t_{k+1}^\sigma - \xi^\sigma)^{\varkappa-1} \mathcal{G}_1(\xi, \mathcal{S}_t) d\xi. \tag{45}$$

Substituing $z = \xi^{\sigma}$, we get

$$\mathcal{S}_t(t_{k+1}) = \mathcal{S}_t(0) + \frac{\sigma^{-\varkappa}}{\Gamma(\varkappa)} \int_0^{t_{k+1}^{\sigma}} (t_{k+1}^{\sigma} - z)^{\varkappa-1} \mathcal{G}_1(z^{1/\sigma}, \mathcal{S}_t(z^{1/\sigma}))dz, \tag{46}$$

equivalently

$$\mathcal{S}_t(t_{k+1}) = \mathcal{S}_t(0) + \frac{\sigma^{-\varkappa}}{\Gamma(\varkappa)} \sum_{j=0}^{k} \int_{t_j^{\sigma}}^{t_{k+1}^{\sigma}} (t_{k+1}^{\sigma} - z)^{\varkappa-1} \mathcal{G}_1(z^{1/\sigma}, \mathcal{S}_t(z^{1/\sigma}))dz. \tag{47}$$

Here, to simulate the integrals from the right-side of equation (47), we apply the trapezoidal quadrature rule for the weight function $(t_{k+1}^{\sigma} - z)^{\varkappa-1}$. We shift the function $\mathcal{G}_1(z^{1/\sigma}, \mathcal{S}_t(z^{1/\sigma}))$ by its piecewise linear interpolants with choosing nodes at the t_j^{σ} $(j = 0, 1, ..., k+1)$, and then we get

$$\int_{t_j^{\sigma}}^{t_{k+1}^{\sigma}} (t_{k+1}^{\sigma} - z)^{\varkappa-1} \mathcal{G}_1(z^{1/\sigma}, \mathcal{S}_t(z^{1/\sigma}))dz \approx \frac{h^{\varkappa}}{\varkappa(\varkappa+1)} \Bigg[\Bigg((k-j)^{\varkappa+1} - (k-j-\varkappa)(k-j+1)^{\varkappa} \Bigg)$$
$$\times \mathcal{G}_1(t_j, \mathcal{S}_t(t_j)) + \Bigg((k-j+1)^{\varkappa+1} - (k-j+\varkappa+1)(k-j)^{\varkappa} \Bigg) \mathcal{G}_1(t_{j+1}, \mathcal{S}_t(t_{j+1})) \Bigg]. \tag{48}$$

Substituing the above approximation into equation (47), we get the corrector formula for $\mathcal{S}_t(t_{k+1}),\ k = 0, 1, ..., \mathbb{N}-1$,

$$\mathcal{S}_t(t_{k+1}) \approx \mathcal{S}_t(0) + \frac{\sigma^{-\varkappa} h^{\varkappa}}{\Gamma(\varkappa+2)} \sum_{j=0}^{k} a_{j,k+1} \mathcal{G}_1(t_j, \mathcal{S}_t(t_j)) + \frac{\sigma^{-\varkappa} h^{\varkappa}}{\Gamma(\varkappa+2)} \mathcal{G}_1(t_{k+1}, \mathcal{S}_t(t_{k+1})), \tag{49}$$

where

$$a_{j,k+1} = \begin{cases} k^{\varkappa+1} - (k-\varkappa)(k+1)^{\varkappa} \quad if \quad j = 0, \\ (k-j+2)^{\varkappa+1} + (k-j)^{\varkappa+1} - 2(k-j+1)^{\varkappa+1} \quad if \ 1 \le j \le k. \end{cases} \tag{50}$$

At the end we aim to change the quantity $\mathcal{S}_t(t_{k+1})$ from the right-side of equation (49) with the predictor term $\mathcal{S}_t^P(t_{k+1})$ that can be calculated by applying the one-step Adams-Bashforth rule to the integral Eqn. (46). We then susbtitute $\mathcal{G}_1(z^{1/\sigma}, \mathcal{S}_t(z^{1/\sigma}))$ by $\mathcal{G}_1(t_j, \mathcal{S}_t(t_j))$ at each integral in equation (47), obtaining

$$\begin{aligned} \mathcal{S}_t^P(t_{k+1}) &\approx \mathcal{S}_t(0) + \frac{\sigma^{-\varkappa}}{\Gamma(\varkappa)} \sum_{j=0}^{k} \int_{t_j^{\sigma}}^{t_{j+1}^{\sigma}} (t_{k+1}^{\sigma} - z)^{\varkappa-1} \mathcal{G}_1(t_j, \mathcal{S}_t(t_j))dz \\ &= \mathcal{S}_t(0) + \frac{\sigma^{-\varkappa} h^{\varkappa}}{\Gamma(\varkappa+1)} \sum_{j=0}^{k} [(k+1-j)^{\varkappa} - (k-j)^{\varkappa}] \mathcal{G}_1(t_j, \mathcal{S}_t(t_j)). \end{aligned} \tag{51}$$

Therefore, our P-C scheme, for approximating $\mathcal{S}_{t_{k+1}} \approx \mathcal{S}_t(t_{k+1})$, is given by

$$\mathcal{S}_{t_{k+1}} \approx \mathcal{S}_t(0) + \frac{\sigma^{-\varkappa} h^{\varkappa}}{\Gamma(\varkappa+2)} \sum_{j=0}^{k} a_{j,k+1} \mathcal{G}_1(t_j, \mathcal{S}_{t_j}) + \frac{\sigma^{-\varkappa} h^{\varkappa}}{\Gamma(\varkappa+2)} \mathcal{G}_1(t_{k+1}, \mathcal{S}_{t_{k+1}}^P), \tag{52}$$

where $\mathcal{S}_{t_j} \approx \mathcal{S}_t(t_j),\ j = 0, 1, ..., k$, and the predicted value $\mathcal{S}^P_{t_{k+1}} \approx \mathcal{S}^P_t(t_{k+1})$ can be simulated as shown in equation (51) with the quantities $a_{j,k+1}$ given in (50). We can repeat this procedure to approximate all equations of system (39). So, the numerical solution formulae for the adopted model (39) can be written as:

$$\begin{aligned}
\mathcal{S}_{t_{k+1}} &\approx \mathcal{S}_t(0) + \frac{\sigma^{-\varkappa}h^{\varkappa}}{\Gamma(\varkappa+2)}\sum_{j=0}^{k} a_{j,k+1}\mathcal{G}_1(t_j, \mathcal{S}_{t_j}) + \frac{\sigma^{-\varkappa}h^{\varkappa}}{\Gamma(\varkappa+2)}\mathcal{G}_1(t_{k+1}, \mathcal{S}^P_{t_{k+1}}),\\
\mathcal{I}_{t_{k+1}} &\approx \mathcal{I}_t(0) + \frac{\sigma^{-\varkappa}h^{\varkappa}}{\Gamma(\varkappa+2)}\sum_{j=0}^{k} a_{j,k+1}\mathcal{G}_2(t_j, \mathcal{I}_{t_j}) + \frac{\sigma^{-\varkappa}h^{\varkappa}}{\Gamma(\varkappa+2)}\mathcal{G}_2(t_{k+1}, \mathcal{I}^P_{t_{k+1}}),\\
\mathcal{Q}_{t_{k+1}} &\approx \mathcal{Q}_t(0) + \frac{\sigma^{-\varkappa}h^{\varkappa}}{\Gamma(\varkappa+2)}\sum_{j=0}^{k} a_{j,k+1}\mathcal{G}_3(t_j, \mathcal{Q}_{t_j}) + \frac{\sigma^{-\varkappa}h^{\varkappa}}{\Gamma(\varkappa+2)}\mathcal{G}_3(t_{k+1}, \mathcal{Q}^P_{t_{k+1}}),\\
\mathcal{R}_{t_{k+1}} &\approx \mathcal{R}_t(0) + \frac{\sigma^{-\varkappa}h^{\varkappa}}{\Gamma(\varkappa+2)}\sum_{j=0}^{k} a_{j,k+1}\mathcal{G}_4(t_j, \mathcal{R}_{t_j}) + \frac{\sigma^{-\varkappa}h^{\varkappa}}{\Gamma(\varkappa+2)}\mathcal{G}_4(t_{k+1}, \mathcal{R}^P_{t_{k+1}}),
\end{aligned} \tag{53}$$

where

$$\begin{aligned}
\mathcal{S}^P_t(t_{k+1}) &\approx \mathcal{S}_t(0) + \frac{\sigma^{-\varkappa}h^{\varkappa}}{\Gamma(\varkappa+1)}\sum_{j=0}^{k}[(k+1-j)^{\varkappa} - (k-j)^{\varkappa}]\mathcal{G}_1(t_j, \mathcal{S}_t(t_j)),\\
\mathcal{I}^P_t(t_{k+1}) &\approx \mathcal{I}_t(0) + \frac{\sigma^{-\varkappa}h^{\varkappa}}{\Gamma(\varkappa+1)}\sum_{j=0}^{k}[(k+1-j)^{\varkappa} - (k-j)^{\varkappa}]\mathcal{G}_2(t_j, \mathcal{I}_t(t_j)),\\
\mathcal{Q}^P_t(t_{k+1}) &\approx \mathcal{Q}_t(0) + \frac{\sigma^{-\varkappa}h^{\varkappa}}{\Gamma(\varkappa+1)}\sum_{j=0}^{k}[(k+1-j)^{\varkappa} - (k-j)^{\varkappa}]\mathcal{G}_3(t_j, \mathcal{Q}_t(t_j)),\\
\mathcal{R}^P_t(t_{k+1}) &\approx \mathcal{R}_t(0) + \frac{\sigma^{-\varkappa}h^{\varkappa}}{\Gamma(\varkappa+1)}\sum_{j=0}^{k}[(k+1-j)^{\varkappa} - (k-j)^{\varkappa}]\mathcal{G}_4(t_j, \mathcal{R}_t(t_j)).
\end{aligned} \tag{54}$$

6.2.1. Stability analysis

Theorem 13. *If $\mathcal{G}_1(t, \mathcal{S}_t)$ satisfies a Lipschitz condition on the second variable and $\mathcal{S}_{t_j}$ $(j = 1, ..., k+1)$ are the solutions of the above approximations (53) and (54). Then, the proposed scheme (53) and (54) are conditionally stable.*

Proof. Let $\tilde{S}_{t_0}$, $\tilde{S}_{t_j}$ $(j = 0, ..., r+1)$ and $S^{\tilde{P}}_{t_{r+1}}$ $(r = 0, ..., N-1)$ be perturbations of S_{t_0}, S_{t_j} and $S^P_{t_{r+1}}$, respectively. Then, the proposed approximation equations are received by analysing Eqs. (53) and (54)

$$S^{\tilde{P}}_{t_{r+1}} = \tilde{S}_{t_0} + \frac{\theta^{-\varkappa}h^{\varkappa}}{\Gamma(\varkappa+1)}\sum_{j=0}^{r} b_{j,r+1}(\mathcal{G}_1(t_j, S_{t_j} + \tilde{S}_{t_j}) - \mathcal{G}_1(t_j, S_{t_j})), \tag{55}$$

here $b_{j,r+1} = [(r+1-j)^{\varkappa} - (r-j)^{\varkappa}]$

$$\begin{aligned}
S_{t_{r+1}} &= \tilde{S}_{t_0} + \frac{\theta^{-\varkappa}h^{\varkappa}}{\Gamma(\varkappa+2)}(\mathcal{G}_1(t_{r+1}, S^P_{t_{r+1}} + S^{\tilde{P}}_{t_{r+1}}) - \mathcal{G}_1(t_{r+1}, S^P_{t_{r+1}})) +\\
&\frac{\theta^{-\varkappa}h^{\varkappa}}{\Gamma(\varkappa+2)}\sum_{j=0}^{r} a_{j,r+1}(\mathcal{G}_1(t_j, S_{t_j} + \tilde{S}_{t_j}) - \mathcal{G}_1(t_j, S_{t_j})),
\end{aligned} \tag{56}$$

Using the Lipschitz condition, we simulate

$$|\tilde{S_{t_{r+1}}}| \leq \zeta_0 + \frac{\theta^{-\varkappa}h^{\varkappa}m_1}{\Gamma(\varkappa+2)}\left(|M^{\tilde{P}}_{r_{r+1}}| + \sum_{j=1}^{r} a_{j,r+1}|\tilde{S_{t_j}}|\right), \tag{57}$$

where $\zeta_0 = \max_{0\leq k\leq N}\{|\tilde{S_{t_0}}| + \frac{\theta^{-\varkappa}h^{\varkappa}m_1a_{r,0}}{\Gamma(\varkappa+2)}|\tilde{S_{t_0}}|\}$. Also, as used in [17], we derive

$$|S^{\tilde{P}}_{t_{r+1}}| \leq \eta_0 + \frac{\theta^{-\varkappa}h^{\varkappa}m_1}{\Gamma(\varkappa+1)}\sum_{j=1}^{r} b_{j,r+1}|\tilde{S_{t_j}}|, \tag{58}$$

where $\eta_0 = \max_{0\leq r\leq N}\{|\tilde{S_{t_0}}| + \frac{\theta^{-\varkappa}h^{\beta}m_1b_{r,0}}{\Gamma(\varkappa+1)}|\tilde{S_{t_0}}|\}$. Substituting $|S^{\tilde{P}}_{t_{r+1}}|$ from Eq. (58) into Eq. (57) results

$$|\tilde{S_{t_{r+1}}}| \leq \gamma_0 + \frac{\theta^{-\varkappa}h^{\varkappa}m_1}{\Gamma(\varkappa+2)}\left(\frac{\theta^{-\varkappa}h^{\varkappa}m_1}{\Gamma(\varkappa+1)}\sum_{j=1}^{r} b_{j,r+1}|\tilde{S_{t_j}}| + \sum_{j=1}^{r} a_{j,r+1}|\tilde{S_{t_j}}|\right), \tag{59}$$

$$\leq \gamma_0 + \frac{\theta^{-\varkappa}h^{\varkappa}m_1}{\Gamma(\varkappa+2)}\sum_{j=1}^{r}\left(\frac{\theta^{-\varkappa}h^{\varkappa}m_1}{\Gamma(\varkappa+1)}b_{j,r+1} + a_{j,r+1}\right)|\tilde{S_{t_j}}|, \tag{60}$$

$$\leq \gamma_0 + \frac{\theta^{-\varkappa}h^{\varkappa}m_1\mathcal{C}_{\varkappa,2}}{\Gamma(\varkappa+2)}\sum_{j=1}^{r}(r+1-j)^{\varkappa-1}|\tilde{S_{t_j}}|, \tag{61}$$

where $\gamma_0 = \max\{\zeta_0 + \frac{\theta^{-\varkappa}h^{\varkappa}m_1a_{r+1,r+1}}{\Gamma(\varkappa+2)}\eta_0\}$. $C_{\varkappa,2}$ is a $+ve$ constant only depends on $\varkappa$ (Lemma 1 used in [17]) and h is supposed to be small enough. Lemma 2 as mentioned in [17] gives $|\tilde{S_{t_{r+1}}}| \leq \mathcal{C}\gamma_0$. which finishes the proof. □

6.3. Graphical results

In this section, we check the correctness of our numerical algorithm by simulating number of graphs at different fractional order values $\varkappa$. Here, we have considered the same initial populations $\mathcal{S}_t(0) = 100, \mathcal{I}_t(0) = 10, \mathcal{Q}_t(0) = 5, \mathcal{R}_t(0) = 0$, and parameter values $d = 0.001, \beta = 0.003, \delta = 0.003, \gamma = 0.002, b = 10, \eta = 0.05, \rho = 0.003, \sigma_1 = 0.003, \sigma_2 = 0.002, q = 1$ as in the CF sense simulations. In the subfigures 5a, 5b, 5c, 5d, we show the variations in $\mathcal{S}_t, \mathcal{I}_t, \mathcal{Q}_t$, and $\mathcal{R}_t$ against the time variable t. Here the variations in the dynamics of the model can be clearly explored at the various derivative order values. We observe that when the fractional order value changes then the differences between phases of the plot lines increase. Also, figure 6 shows the relations between the given classes at various values of $\varkappa$. More concretely, in subfigure 6a we plot the variations $\mathcal{S}_t$ versus $\mathcal{I}_t$, and in 6b we graph the variations $\mathcal{S}_t$ versus $\mathcal{Q}_t$. Meanwhile, in subfigure 6c we plot the variations $\mathcal{S}_t$ versus $\mathcal{R}_t$, and in 6d we plot the variations $\mathcal{R}_t$ versus $\mathcal{I}_t$. The fractional order values which we used here are $\varkappa = 0.75, 0.85, 0.95, 1$ as in the case of CF.

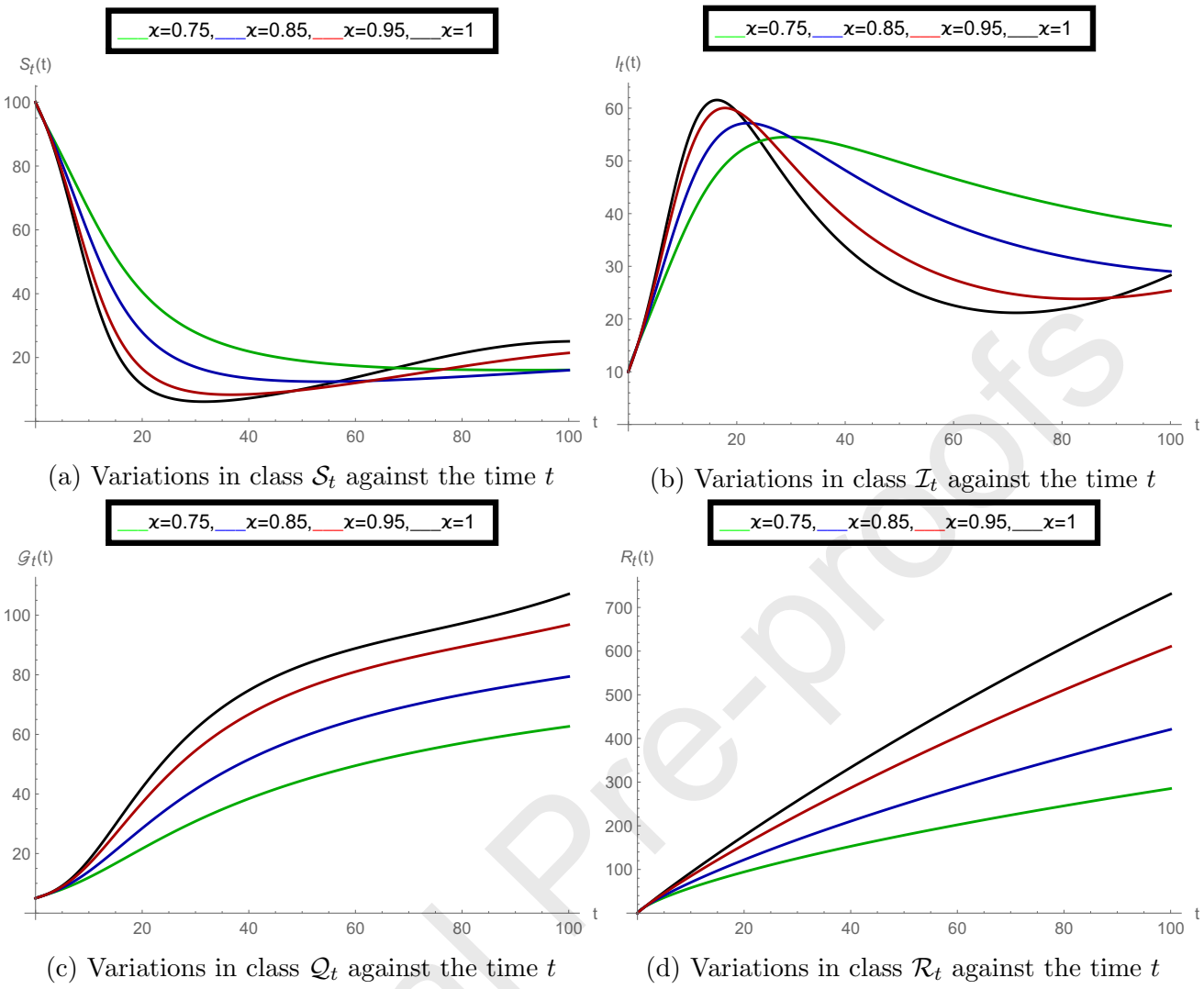

(a) Variations in class $\mathcal{S}_t$ against the time t

(b) Variations in class $\mathcal{I}_t$ against the time t

(c) Variations in class $\mathcal{Q}_t$ against the time t

(d) Variations in class $\mathcal{R}_t$ against the time t

Figure 5: Structure of the model classes in modified Caputo sense at various values of order $\varkappa$, when vaccination fraction $q = 1$.

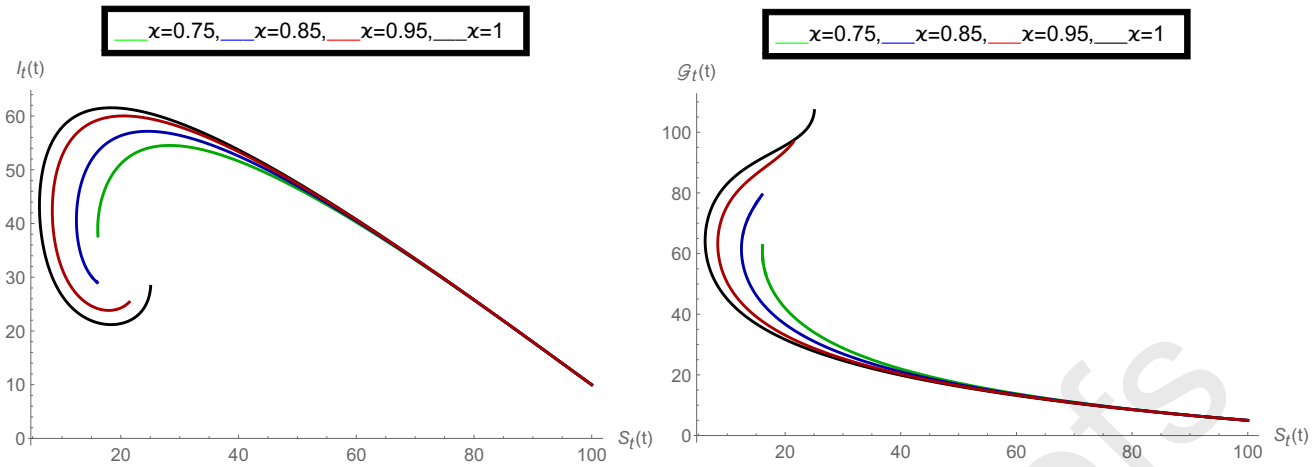

(a) Plot of $\mathcal{S}_t$ versus $\mathcal{I}_t$

(b) Plot of $\mathcal{S}_t$ versus $\mathcal{Q}_t$

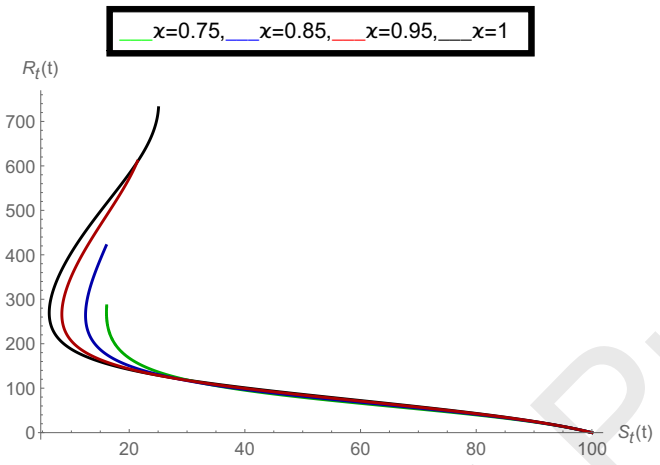

(c) Plot of $\mathcal{S}_t$ versus $\mathcal{R}_t$

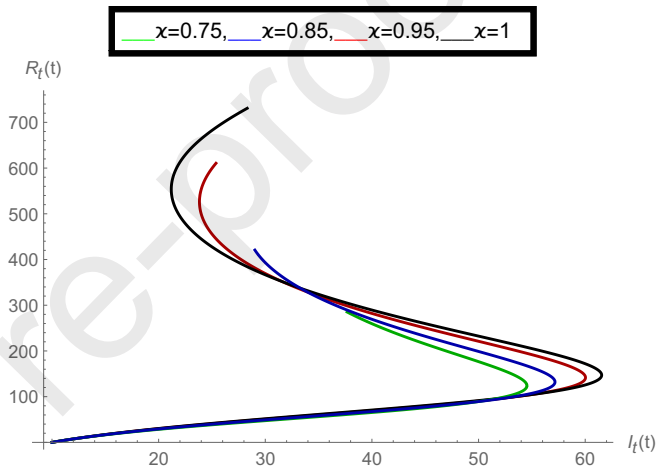

(d) Plot of $\mathcal{R}_t$ versus $\mathcal{I}_t$

Figure 6: Variations in the model classes compare to each other, when vaccination fraction $q = 1$.

Now, to simulate the role of vaccine on the proposed modified Caputo model classes, we change the value of the vaccination fraction q. Here, in the family of Figure 7, the subfigures 7a, 7b, 7c, 7d demonstrate the variations in $\mathcal{S}_t, \mathcal{I}_t, \mathcal{Q}_t$, and $\mathcal{R}_t$ against the time variable t at the vaccination fraction $q = 0$, where all other values are same as used above. Similarly, Figure 8 demonstrates the changes in the model classes when the vaccination rate $q = 0.5$. By the comparison of Figure 7 and 8, we can easily observe that when the value of vaccination fraction q increases then the population of infectious humans decreases. This clearly means that high vaccine rate gives much safety and become the only way to control the COVID-19. Now, as many countries like India, USA, UK, Spain, and Brazil have a good rate of vaccination which is a strong answer against COVID-19 infection. Vaccine availability alongwith quarantine and other optimal control facilities makes these countries much stronger to fight against this virus.

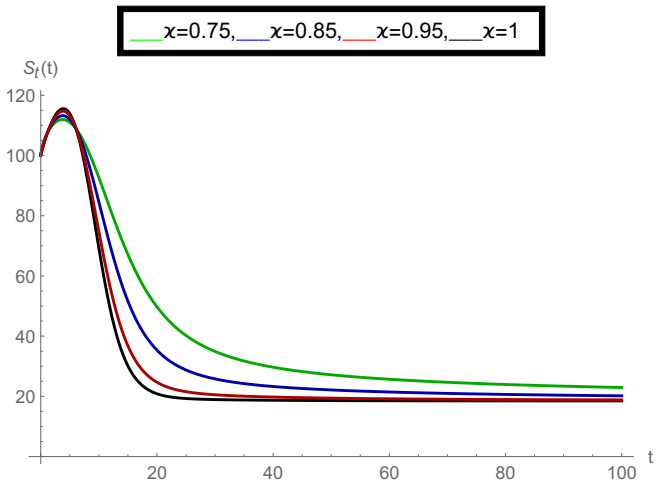

(a) Variations in class $\mathcal{S}_t$ against the time t

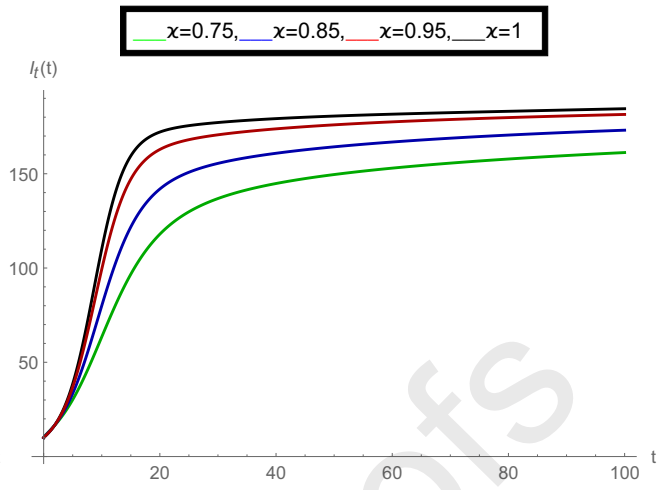

(b) Variations in class $\mathcal{I}_t$ against the time t

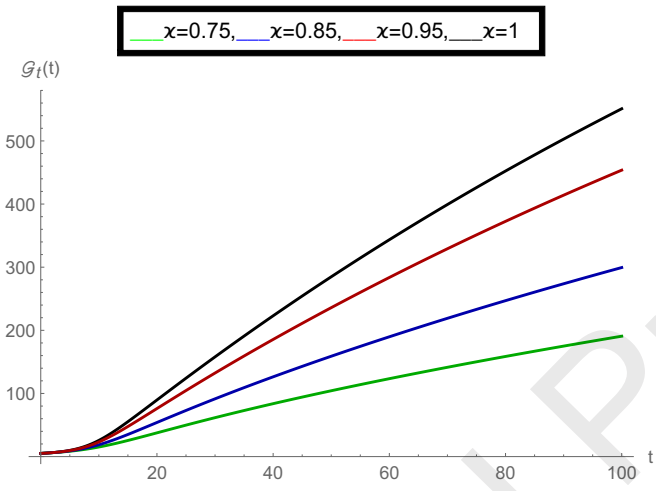

(c) Variations in class $\mathcal{Q}_t$ against the time t

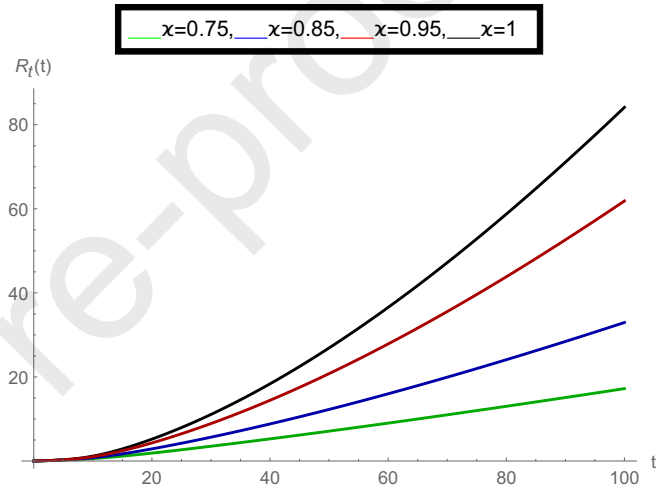

(d) Variations in class $\mathcal{R}_t$ against the time t

Figure 7: Structure of the model classes in CF sense at various values of order $\varkappa$, when vaccination fraction $q = 0$.

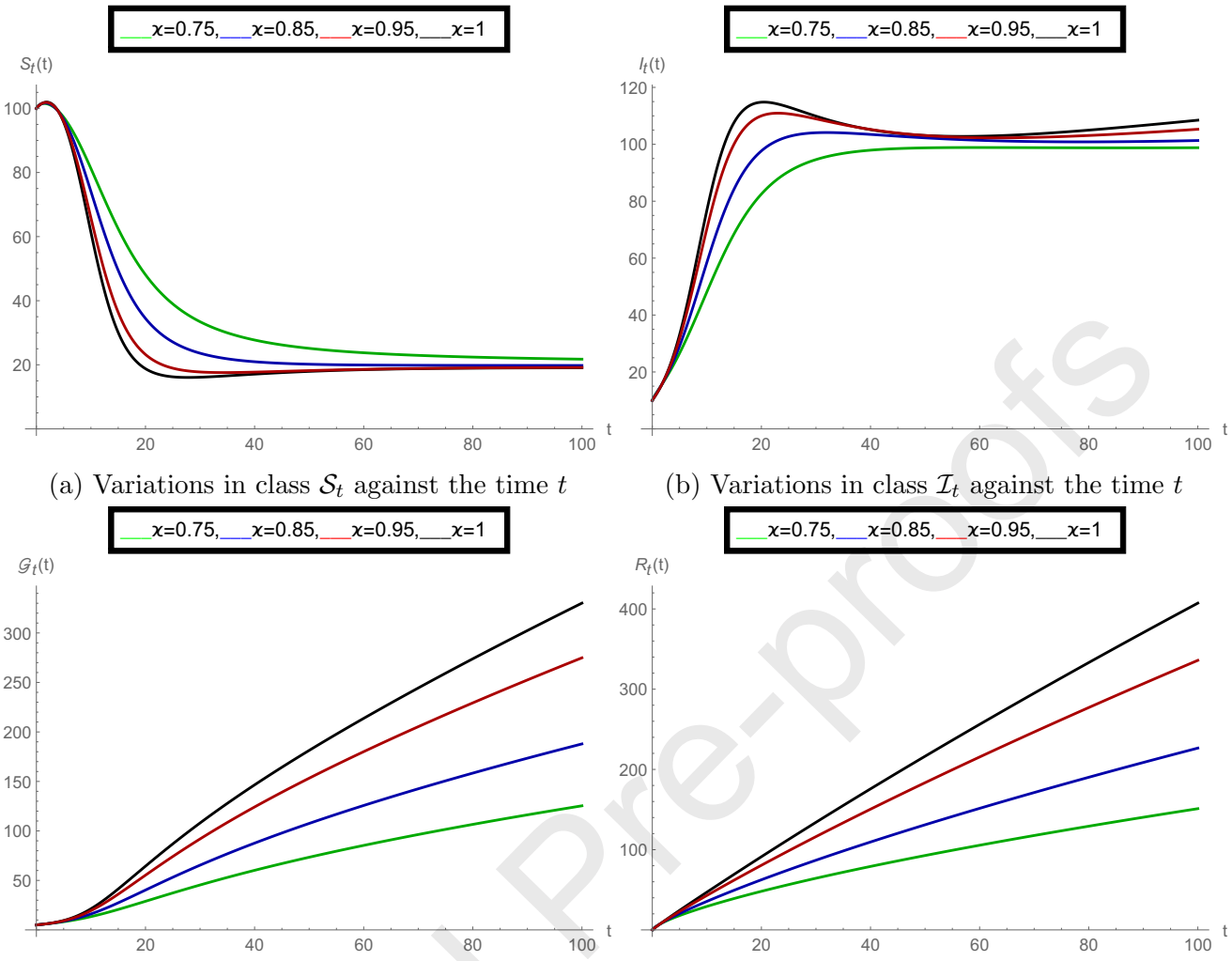

(a) Variations in class $\mathcal{S}_t$ against the time t

(b) Variations in class $\mathcal{I}_t$ against the time t

(c) Variations in class $\mathcal{Q}_t$ against the time t

(d) Variations in class $\mathcal{R}_t$ against the time t

Figure 8: Structure of the model classes in CF sense at various values of order $\varkappa$, when vaccination fraction $q = 0.5$.

From the given graphical observations, we can observe that the both kernel properties (exponential decay kernel in CF sense and singular kernel in modified Caputo sense) work well to study the given COVID-19 epidemic dynamics. All graphs are performed by using *Mathematica* software. The variations in the separate classes for both derivatives which are given in Figures 1 and 5 are probably same but the dynamics of the given classes slightly change. This fact can be observed comparing the group of Figures 2 and 6. It is clearly observed that vaccination fraction q plays a very important role in the given dynamics and increment in the vaccine rate can decrease the Covid-19 infection.

7. Conclusion

In this study, two new non-classical COVID-19 epidemic models have been proposed. As a novelty, we include vaccine rate. First we have proposed a classical order model and then we have justified the fractional-order models by analysing the positivity and boundedness of solutions. The disease-free and endemic equilibrium points are calculated along with basic reproductive number. We have satisfied the existence of unique solution for both

variable order Caputo-Fabrizio and generalised Caputo-type fractional models. We used two different fractional numerical algorithms along with their stability analysis to solve the proposed models. A deep and long discussion on graphical simulations is given making use of *Mathematica* software. The current study provides a description of the propagation of COVID-19 disease and supporting analysis proves the correctness of our results. In future, the current model can be validated by using real data from different countries. Also, some other fractional derivatives can be used to solve the current dynamical model.

Conflict of interest

Current work does not have any conflicts of interest.

Funding

This research was funded by the Science, Research and Innovation Promotion Fund under Basic Research Plan-Saun Dusit University, Thailand.

CRediT authorship contribution statement

All authors equally contributed to this work.

References

[1] Bekiros, S. & Kouloumpou, D. (2020). SBDiEM: A new mathematical model of infectious disease dynamics. Chaos, Solitons & Fractals, 136, 109828.

[2] Bocharov, G., Volpert, V., Ludewig, B. & Meyerhans, A. (2018). Mathematical Immunology of Virus Infections. Springer International Publishing.

[3] Brauer, F., Driessche, P. Van. den. & Wu, J. (2008). Mathematical Epidemiology. Springer Berlin Heidelberg.

[4] Brauer, F. (2017). Mathematical epidemiology: Past, present, and future. Infectious Disease Modelling 2, 113-127.

[5] Zaman, G., Jung, H., Torres, D. F. M. & Zeb, A. (2017). Mathematical Modeling and Control of Infectious Diseases. Computational and Mathematical Methods in Medicine, 7149154, 1 page.

[6] Higazy, M. (2020). Novel fractional order SIDARTHE mathematical model of COVID-19 pandemic, Chaos, Solitons & Fractals, 138, 110007.

[7] Zeb, A., Alzahrani, E., Erturk, V. S. & Zaman, G. (2020). Mathematical Model for Coronavirus Disease 2019 (COVID-19) Containing Isolation Class. BioMed Research International, https://doi.org/10.1155/2020/3452402.

[8] Zhang, Z., Zeb, A., Alzahrani, E. & Iqbal, S. (2020) Crowding effects on the dynamics of COVID-19 mathematical model. Advances in Difference Equations, 2020 (1), 1–13.

[9] Zhang, Z., Zeb,, A., Hussain, S. & Alzahrani, E. (2020). Dynamics of COVID-19 mathematical model with stochastic perturbation. Advances in Difference Equations, 2020 (1), 1–12.

[10] Atangana, A. & Iğret Araz S. (2021). Modeling and forecasting the spread of COVID-19 with stochastic and deterministic approaches: Africa and Europe. Adv. Difference Equ. (2021), 57–107.

[11] Mahrouf, M., Boukhouima, A., Zine, H., Lotfi, E. M., Torres, D. F. M. & Yousfi, N. (2021). Modeling and forecasting of COVID-19 spreading by delayed stochastic differential equations. Axioms 10 (1), 16 pp.

[12] Abboubakar, H., Kumar, P., Erturk, V.S. & Kumar, A. (2021). A mathematical study of a Tuberculosis model with fractional derivatives. International Journal of Modeling, Simulation, and Scientific Computing.

[13] Abboubakar, H., Kumar, P., Rangaig, N., & Kumar, S. (2020). A Malaria Model with Caputo-Fabrizio and Atangana-Baleanu Derivatives. International Journal of Modeling, Simulation, and Scientific Computing.

[14] Gao, W., Veeresha, P., Baskonus, H. M., Prakasha, D. G. & Kumar, P. (2020). A New Study of Unreported Cases of 2019-nCOV Epidemic Outbreaks. Chaos, Solitons & Fractals, 109929.

[15] Kumar, P. & Erturk, V.S. (2021). A case study of Covid-19 epidemic in India via new generalised Caputo type fractional derivatives. Mathematical Methods in the Applied Sciences, 1–14.

[16] Kumar, P. & Erturk, V.S. The analysis of a time delay fractional COVID-19 model via Caputo type fractional derivative, Mathematical Methods in the Applied Sciences.

[17] V.S. Erturk and P. Kumar, Solution of a COVID-19 model via new generalized Caputo-type fractional derivatives, Chaos, Solitons & Fractals, 2020, 110280.

[18] Kumar, P., Erturk, V.S., Abboubakar, H. & Nisar, K.S. (2021). Prediction studies of the epidemic peak of coronavirus disease in Brazil via new generalised Caputo type fractional derivatives. Alexandria Engineering Journal, 60(3), 3189-3204.

[19] Nabi, K.N., Abboubakar, H. & Kumar, P. (2020). Forecasting of COVID-19 pandemic: From integer derivatives to fractional derivatives. Chaos, Solitons & Fractals, 110283.

[20] Nabi, K.N., Kumar, P. & Erturk, V.S. (2021). Projections and fractional dynamics of COVID-19 with optimal control strategies. Chaos, Solitons & Fractals, 110689.

[21] Kumar P. & Erturk, V.S. (2021). Environmental persistence influences infection dynamics for a butterfly pathogen via new generalised Caputo type fractional derivative. Chaos, Solitons & Fractals, 144, 110672.

[22] Caputo, M. & Mauro, F. (2015). A new definition of fractional derivative without singular kernel. Progr. Fract. Differ. Appl, 1(2), 1–13.

[23] Verma, P. & Kumar, M. (2020). Analysis of a novel coronavirus (2019-nCOV) system with variable Caputo-Fabrizio fractional order. Chaos, Solitons & Fractals, 110451.

[24] Odibat, Z.M., & Shawagfeh, N.T. (2007). Generalized Taylor's formula. *Appl. Math. Comput.,* 186(1) 286–293.

[25] Oldham, K. & Spanier, J. The fractional calculus theory and applications of differentiation and integration to arbitrary order. Elsevier Science, 1974.

[26] Podlubny, I. Fractional differential equations: an introduction to fractional derivatives, fractional differential equations, to methods of their solution and some of their applications. Academic Press, 1998.

[27] Rudolf, H. Applications of fractional calculus in physics. 2000.

[28] Kilbas, A. A., Srivastava, H. M., & Trujillo, J. J. Theory and applications of fractional differential equations. Amsterdam ; Boston : Elsevier, 2006.

[29] Odibat, Z., & Baleanu, D. (2020). Numerical simulation of initial value problems with generalized Caputo-type fractional derivatives. Applied Numerical Mathematics, 156, 94-105.

[30] Naik, P. A., Yavuz, M., Qureshi, S., Zu, J., & Townley, S. (2020). Modeling and analysis of COVID-19 epidemics with treatment in fractional derivatives using real data from Pakistan. The European Physical Journal Plus, 135(10), 1-42.

[31] Yavuz, M., Coar, F. ., Gnay, F., & zdemir, F. N. (2021). A new mathematical modeling of the COVID-19 pandemic including the vaccination campaign. Open Journal of Modelling and Simulation, 9(3), 299-321.

[32] Naik, P. A., Owolabi, K. M., Yavuz, M., & Zu, J. (2020). Chaotic dynamics of a fractional order HIV-1 model involving AIDS-related cancer cells. Chaos, Solitons & Fractals, 140, 110272.

[33] Hammouch, Z., Yavuz, M., & zdemir, N. (2021). Numerical Solutions and Synchronization of a Variable-Order Fractional Chaotic System. Mathematical Modelling and Numerical Simulation with Applications (MMNSA), 1(1), 11-23.

[34] Yavuz, M., & Sene, N. (2020). Stability analysis and numerical computation of the fractional predatorprey model with the harvesting rate. Fractal and Fractional, 4(3), 35.

[35] Naik, P. A., Yavuz, M., & Zu, J. (2020). The role of prostitution on HIV transmission with memory: A modeling approach. Alexandria Engineering Journal, 59(4), 2513-2531.

[36] Yavuz, M., & zdemir, N. (2020). Analysis of an epidemic spreading model with exponential decay law. Mathematical Sciences and Applications E-Notes, 8(1), 142-154.

[37] Bonyah, E., Yavuz, M., Baleanu, D., & Kumar, S. (2021). A robust study on the listeriosis disease by adopting fractal-fractional operators. Alexandria Engineering Journal.

[38] Odibat, Z., Erturk, V. S., Kumar, P., & Govindaraj, V. (2021). Dynamics of generalized Caputo type delay fractional differential equations using a modified Predictor-Corrector scheme. Physica Scripta, 96(12), 125213.

[39] Kumar, P., Erturk, V. S., Murillo-Arcila, M., Banerjee, R., & Manickam, A. (2021). A case study of 2019-nCOV cases in Argentina with the real data based on daily cases from March 03, 2020 to March 29, 2021 using classical and fractional derivatives. Advances in Difference Equations, 2021(1), 1-21.

[40] Kalaiselvi, R., Manickam, A., Agrawal, M., & Kumar, P. (2021). A Study of Mathematical Model for Extended Lognormal Distribution to Obligatory Role of Hypothalamic Neuroestradiol during the Estrogen induced LH surge in Female Ovariectomized Rhesus Monkey. Annals of the Romanian Society for Cell Biology, 4122-4127.